PET Basics
(with some SPECT features as well)

Mika Teräs
Chief Physicist, Dep of Medical Physics, TUH
Professor, Institute of Biomedicine, UTU

Turku PET Centre

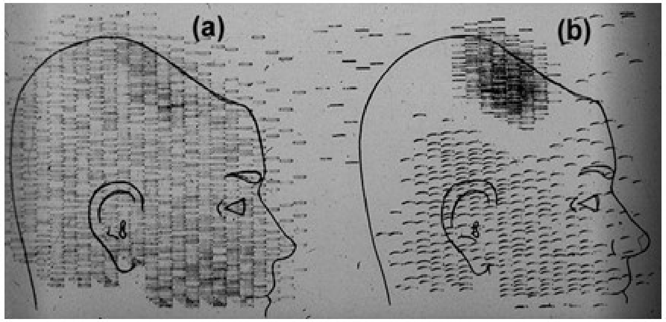

Figure 2: Coincidence and unbalance scans of patient with recurring brain tumor. Coincidence scan (a) of a patient showing recurrence of tumor under previous operation site, and unbalance scan (b) showing asymmetry to the left. (Reproduced from Brownell and Sweet 1953 [8]).

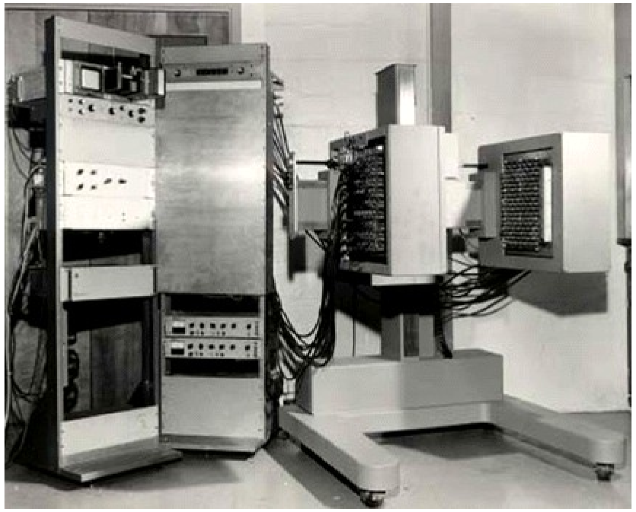

PC-I, the first tomographic PET

BROWNELL et al.
``Quantitative dynamic studies using short-lived radioisotopes and positron detection" in *Proceedings of the Symposium on Dynamic Studies with Radioisotopes in Medicine*, Rotterdam. August 31 - September 4, 1970. IAEA. **Vienna. 1971. pp. 161-172**.

Astro-Medical Imaging
Turku 12.5.2022

Quantitative Imaging Biomarkers Alliance

Entire chain of process determines quantitative result of an imaging biomaker

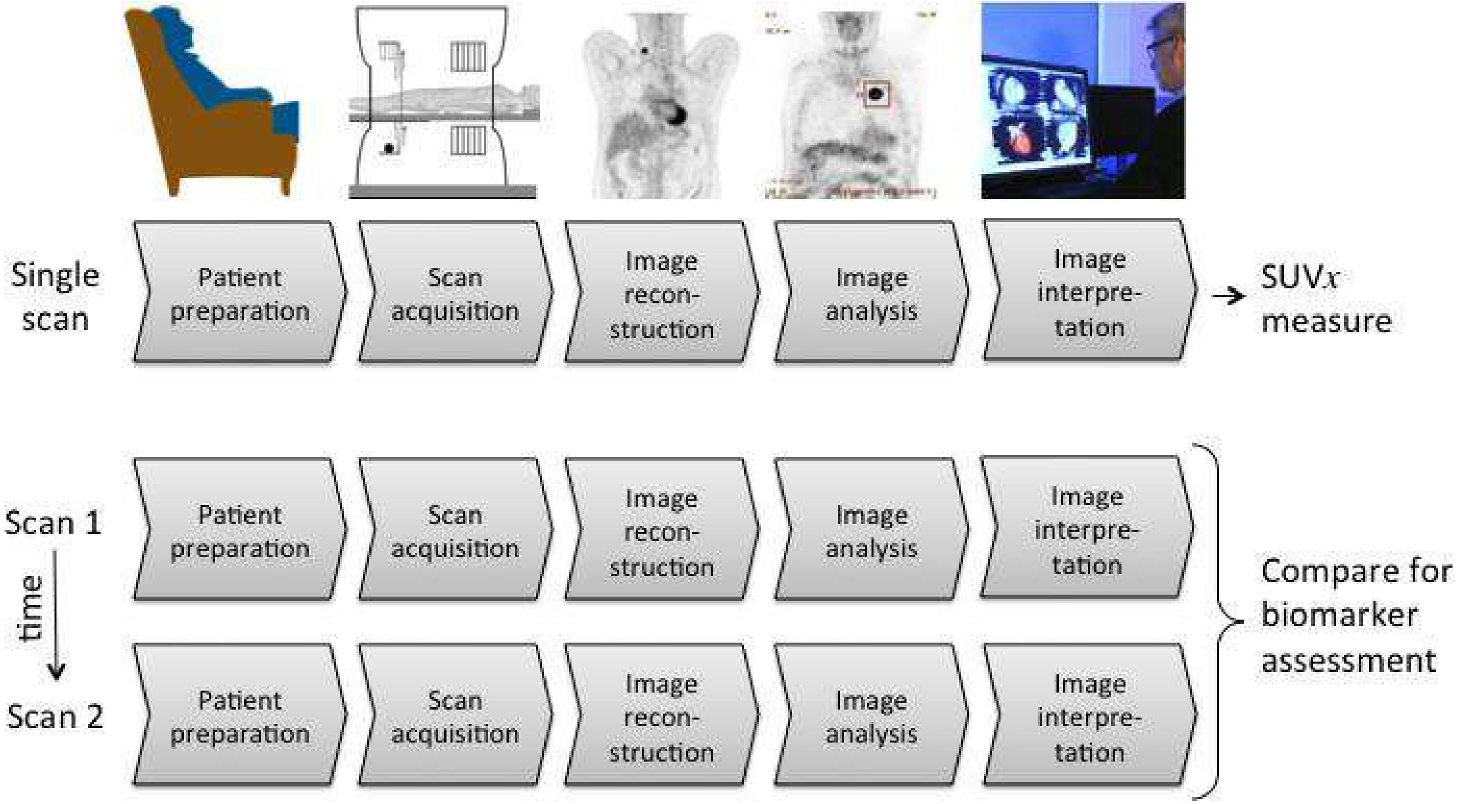

Single scan

Patient preparation → Scan acquisition → Image recon-struction → Image analysis → Image interpre-tation → SUVx measure

Scan 1

Patient preparation → Scan acquisition → Image recon-struction → Image analysis → Image interpre-tation

time

Scan 2

Patient preparation → Scan acquisition → Image recon-struction → Image analysis → Image interpre-tation

Compare for biomarker assessment

Picture taken from QIBA FDG PET/CT profile (www.**RSNA.ORG/QIBA**)

The role of medical imaging modalities

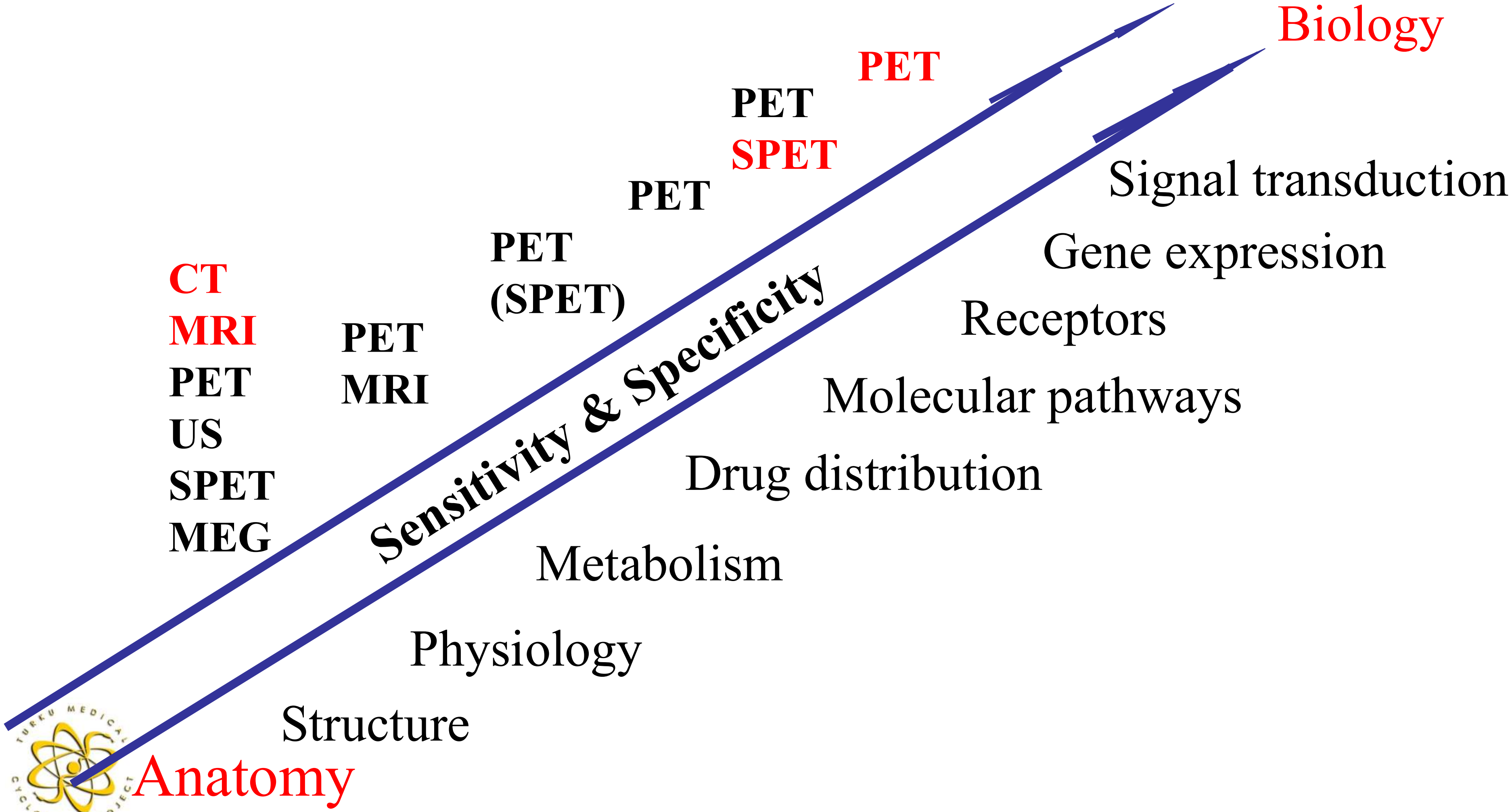

CT
MRI
PET
US
SPET
MEG

PET
MRI

PET
(SPET)

PET

PET
SPET

PET

Sensitivity & Specificity

Anatomy

Structure

Physiology

Metabolism

Drug distribution

Molecular pathways

Receptors

Gene expression

Signal transduction

Biology

Why Multimodality?

Some benefits

- ☐ Better anatomical definition of (S)PET for reading
- ☐ Precise attenuation correction (AC) for quantification
- ☐ Anatomy based Partial Volume correction (PVC)
- ☐ New motion correction (MoCo) algorithms

Example: PET-based hybrid imaging

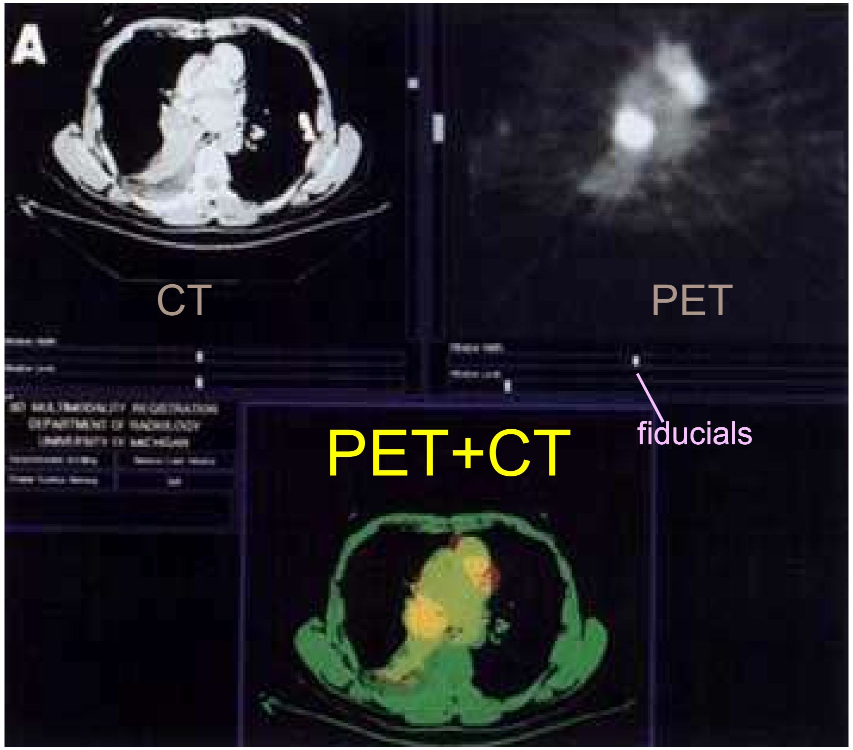

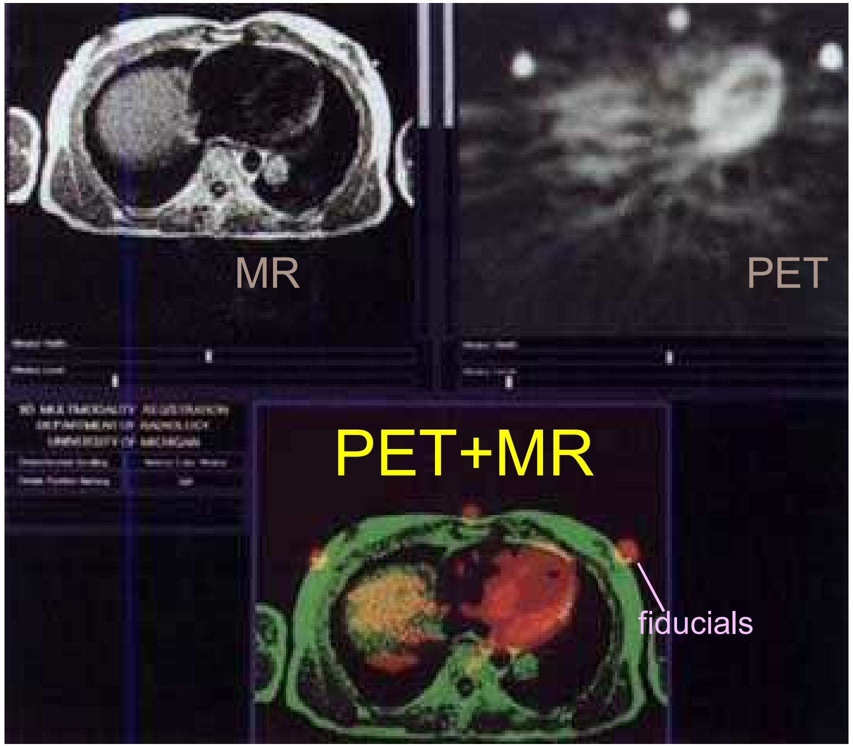

"… Anatometabolic fusion images made using this reasonably simple method [external fiducial landmarks] should prove useful in the management of patients with cancer and other diseases. …" Wahl R et al, JNM 34, 1993

Anato-metabolic imaging = Complementary imaging

Physics - Identification

- ❑ **Detection** (up to 511 keV)
    - ▪ Detector properties
    - ▪ Electronics (speed, data handling)
- ❑ **Imaging**
    - ▪ Choice of modality
        - availability
        - Patient dose, ALARA
    - ▪ Choice of biomarker
    - ▪ Imaging protocol (patient preparation)
- ❑ **Image reconstruction**
    - ▪ Algorithms
    - ▪ Corrections (psf→ PV, motion)

- ❑ Modelling
    - ▪ Quantification
    - ▪ Signalling
    - ▪ Uncertainty analysis
- ❑ Standardisation
    - ▪ National
    - ▪ Global
- ❑ Big Data
    - ▪ National PACS
    - ▪ Bio banks
    - ▪ Reference databases
    - ▪ Automated analysis

Single Photon Emission Tomography (SPET) with CT leaping towards PET quantitation?

Mediso AnyScan SPET / CT / PET GE Discovery NM/CT 670 Pro

Siemens Symbia Intevo Philips Brightview

CT-AC in SPET

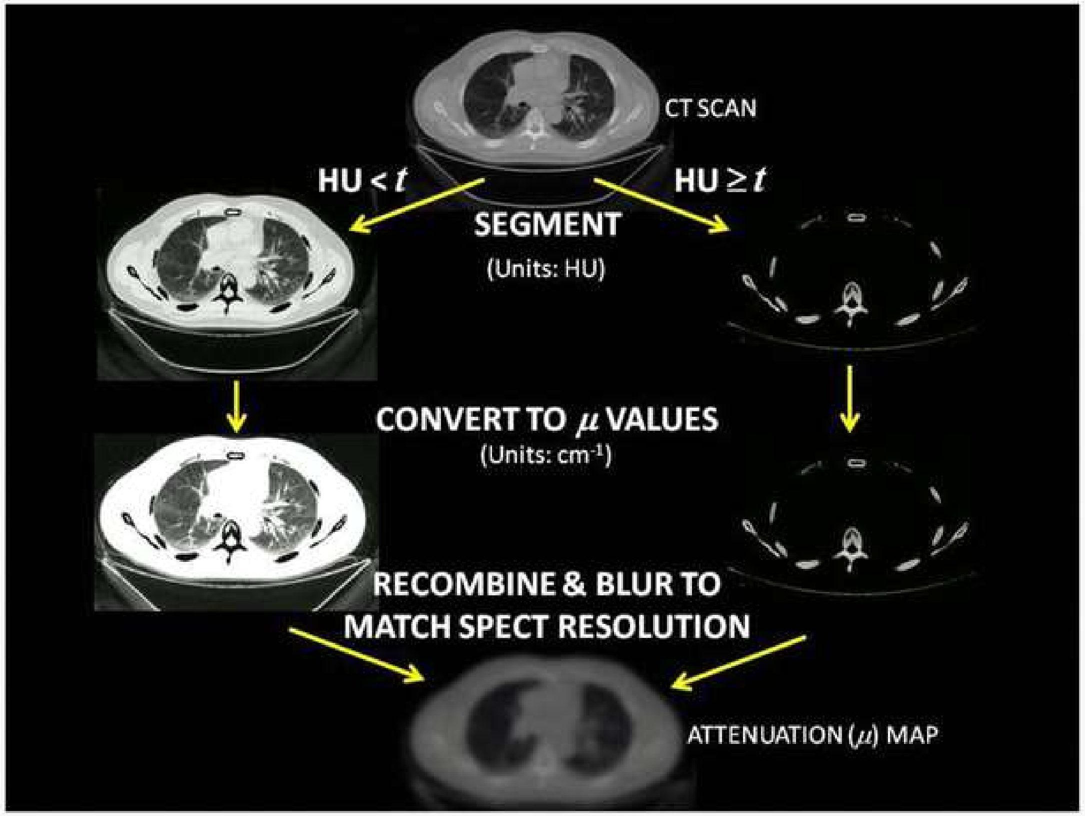

Fig. 5

The steps involved in converting from a CT scan to linear attenuation map are shown. The threshold value t is usually chosen in the range 0–100 HU

Eur J Nucl Med Mol Imaging. 2014 May;41 Suppl 1:S17-25. doi: 10.1007/s00259-013-2542-4. Epub 2013 Sep 14.

Quantitative SPECT/CT: SPECT joins PET as a quantitative imaging modality.

Bailey DL[1], Willowson KP.

Quantitative SPET

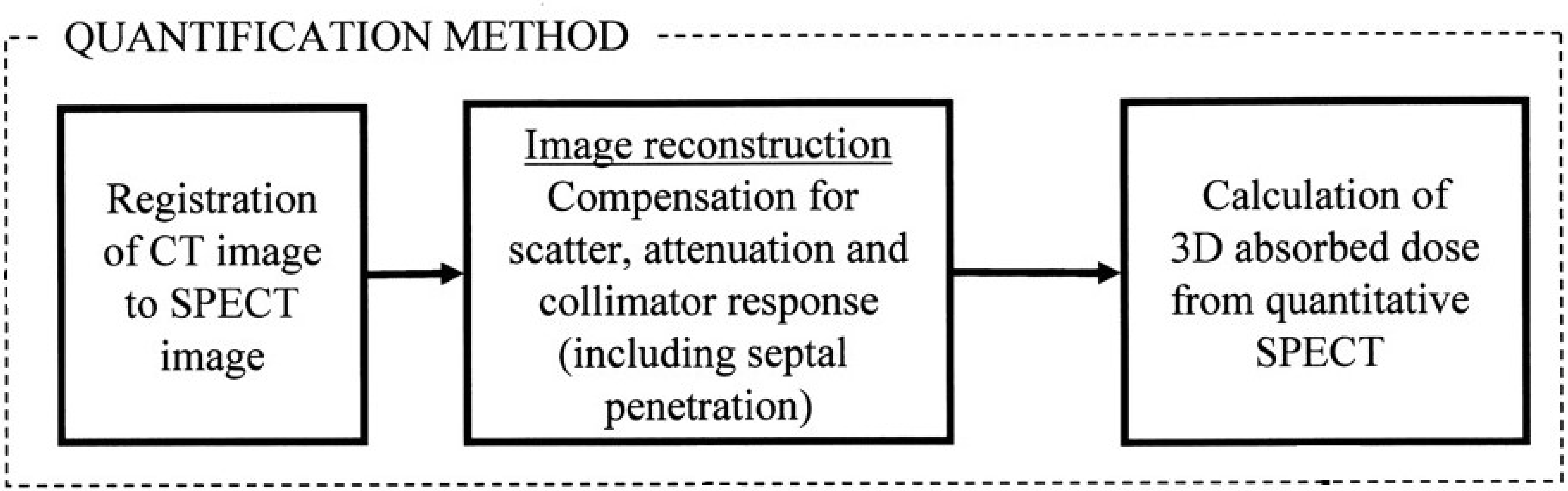
QUANTIFICATION METHOD

Registration of CT image to SPECT image

Image reconstruction
Compensation for scatter, attenuation and collimator response (including septal penetration)

Calculation of 3D absorbed dose from quantitative SPECT

Michael Ljungberg, J Nucl Med 2002; 43:1101–1109

Quantitative SPET - corrections

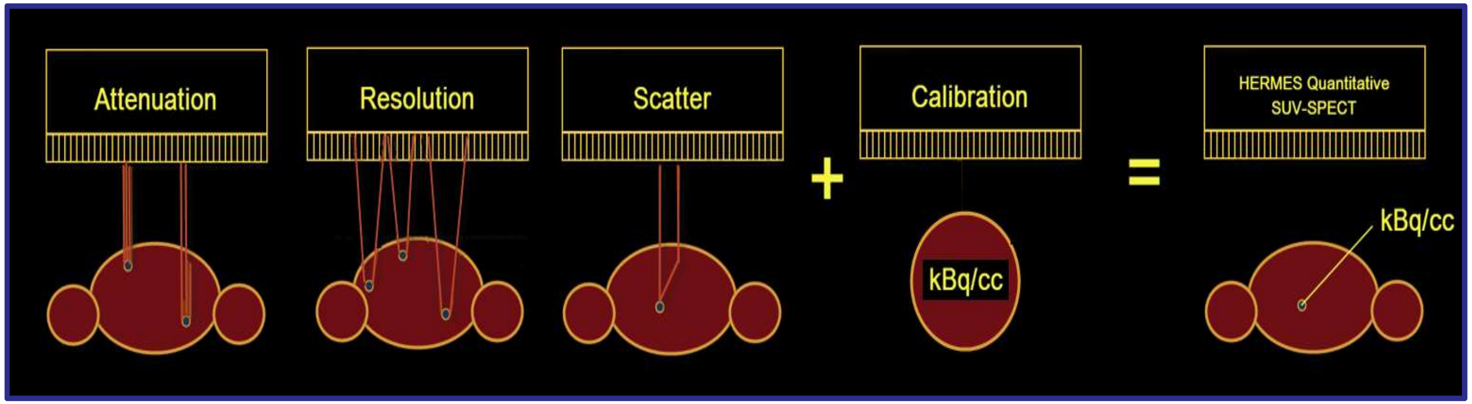

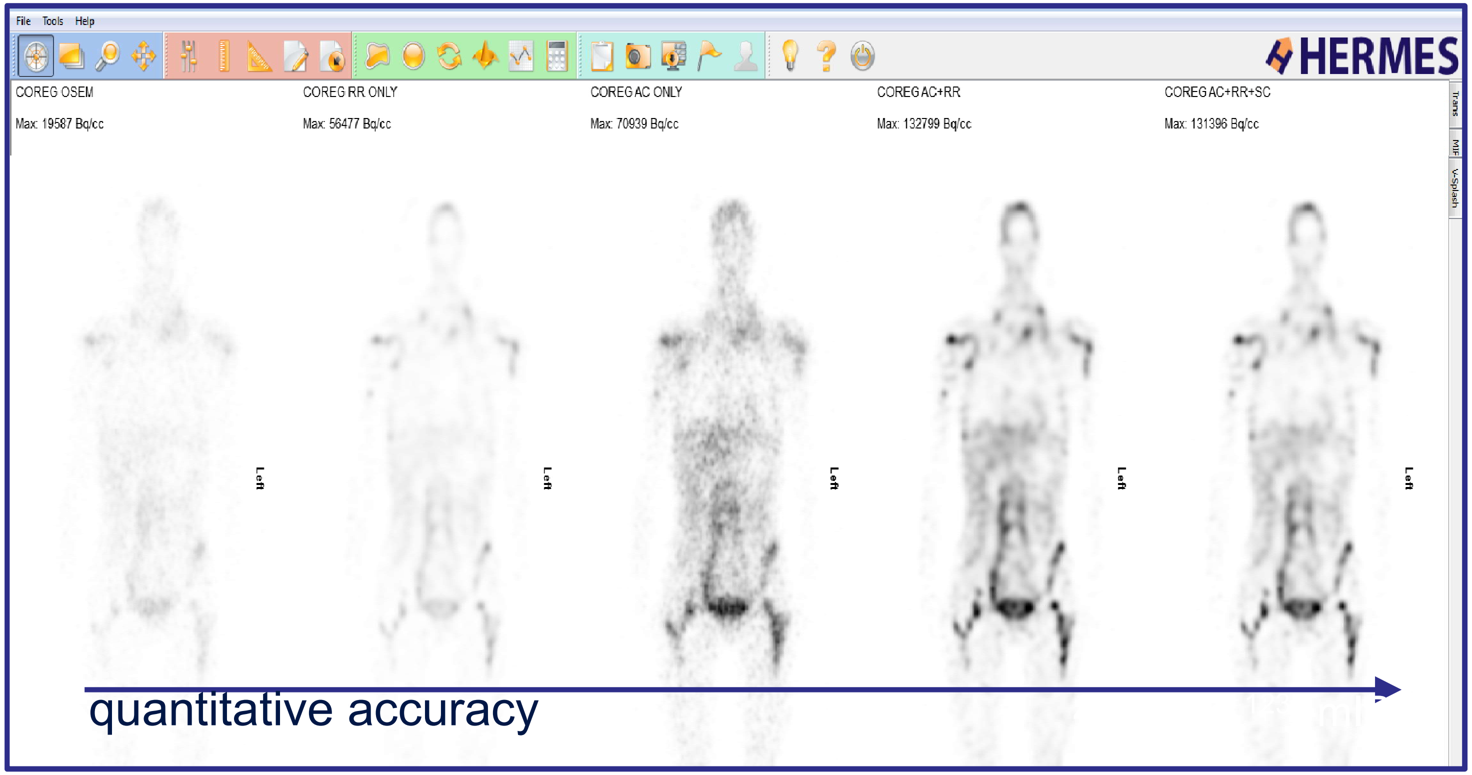

COREG OSEM Max: 19587 Bq/cc

COREG RR ONLY Max: 56477 Bq/cc

COREG AC ONLY Max: 70939 Bq/cc

COREG AC+RR Max: 132799 Bq/cc

COREG AC+RR+SC Max: 131396 Bq/cc

quantitative accuracy

xSPET reconstruction

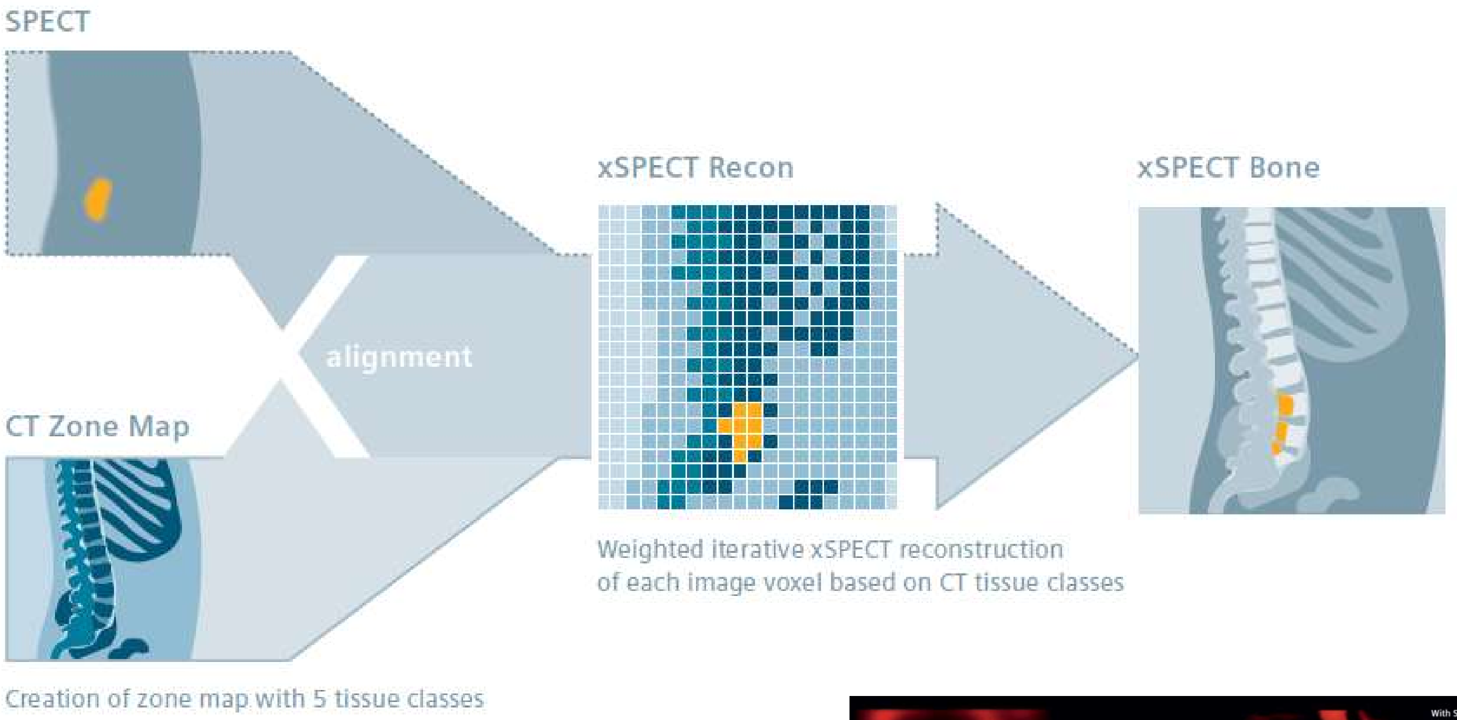

SPECT

alignment

CT Zone Map

Creation of zone map with 5 tissue classes

xSPECT Recon

Weighted iterative xSPECT reconstruction
of each image voxel based on CT tissue classes

xSPECT Bone

SIEMENS

With Symbia Intevo, physicians are now able to have more diagnostic information to aid them in differentiating cancer from other forms of disease.

NaI+PMT vs new CZT detector

Anger-camera

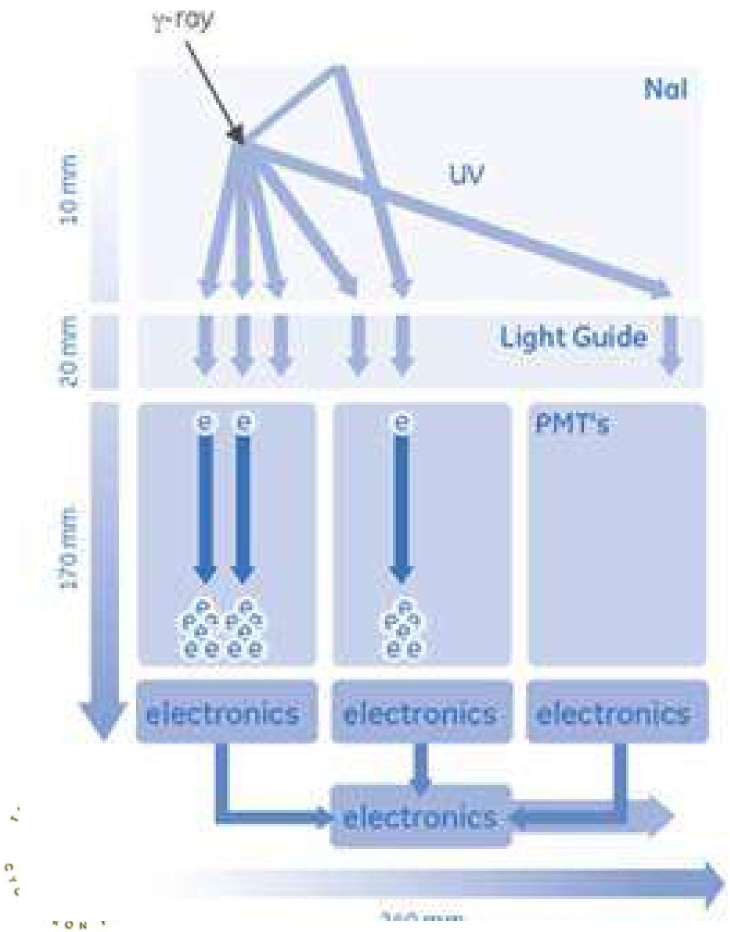

CZT-camera

^{99m}Tc (140keV)

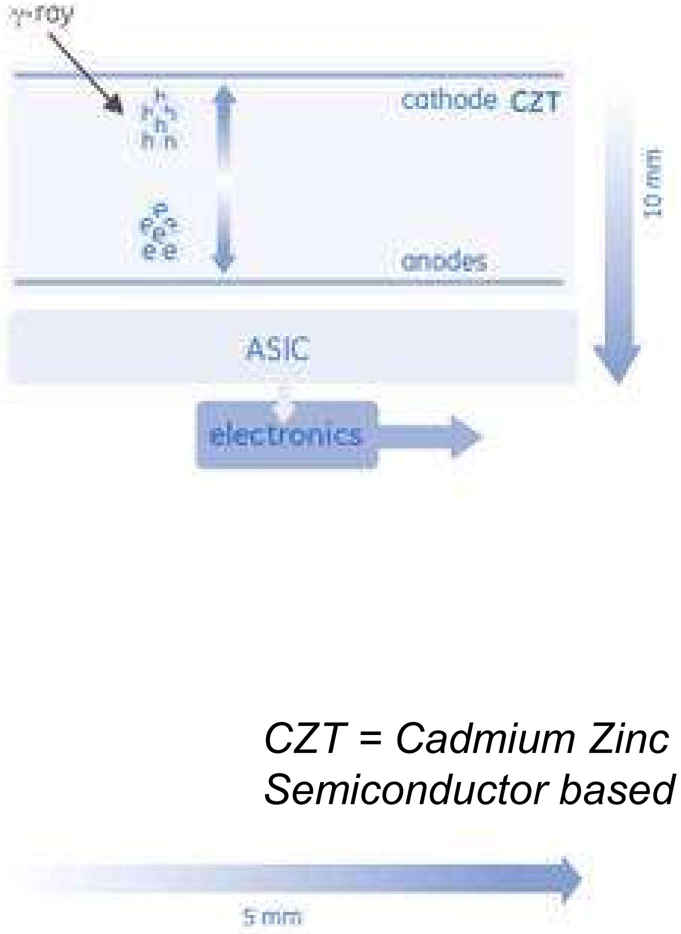

CZT = Cadmium Zinc Telluride
Semiconductor based detector

NaI+PMT vs CZT

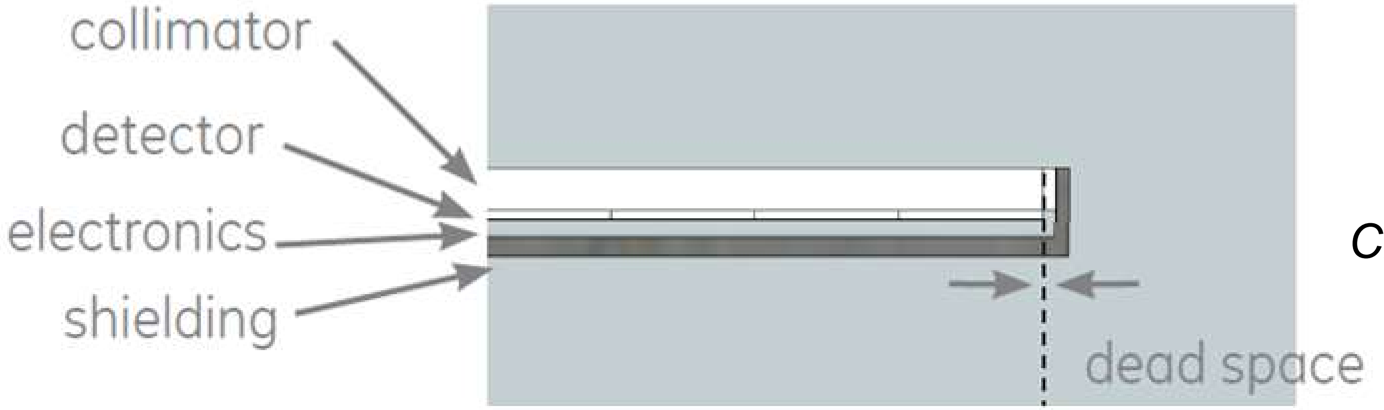

CZT

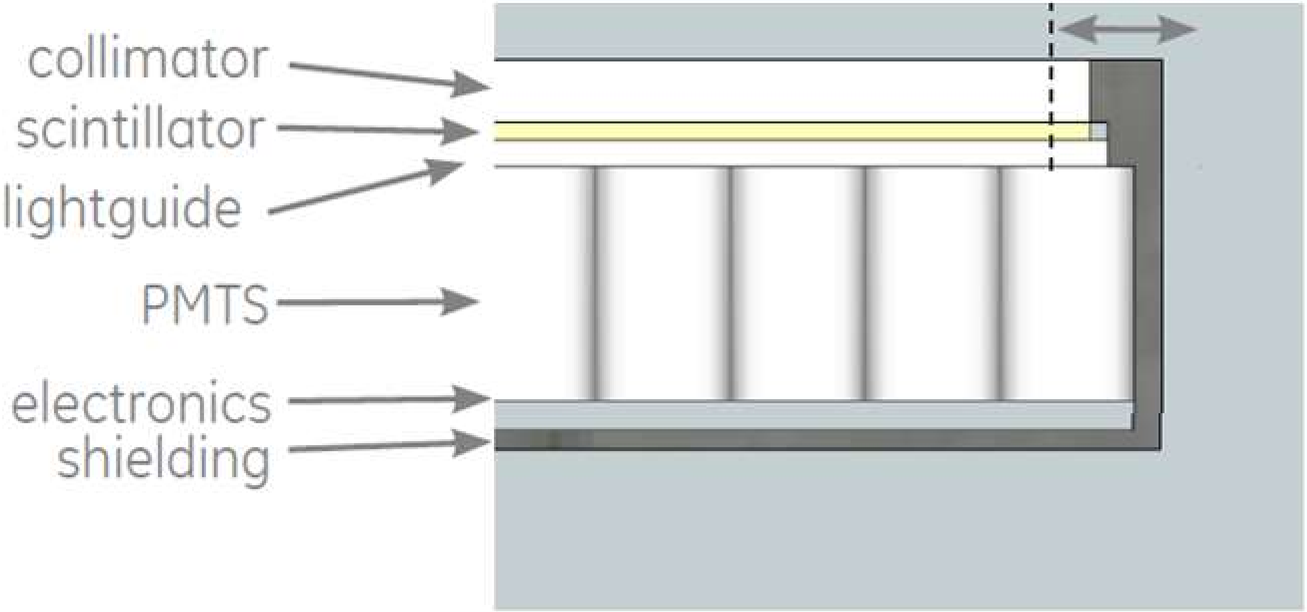

NaI+PMT

CZT- SPET/CT – near future

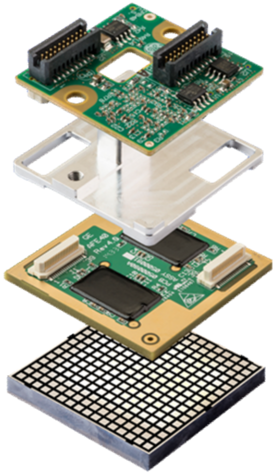

GE Discovery NM/CT 670 CZT
Installed at TUH in late 2017

[StarGuide | GE Healthcare (United States)](https://www.gehealthcare.com/products/molecular-imaging/starguide)

https://www.gehealthcare.com/products/molecular-imaging/starguide

To be installed at TUH in late 2022

https://youtu.be/5acP6VyVEH4

Energy resolution (NaI vs CZT)

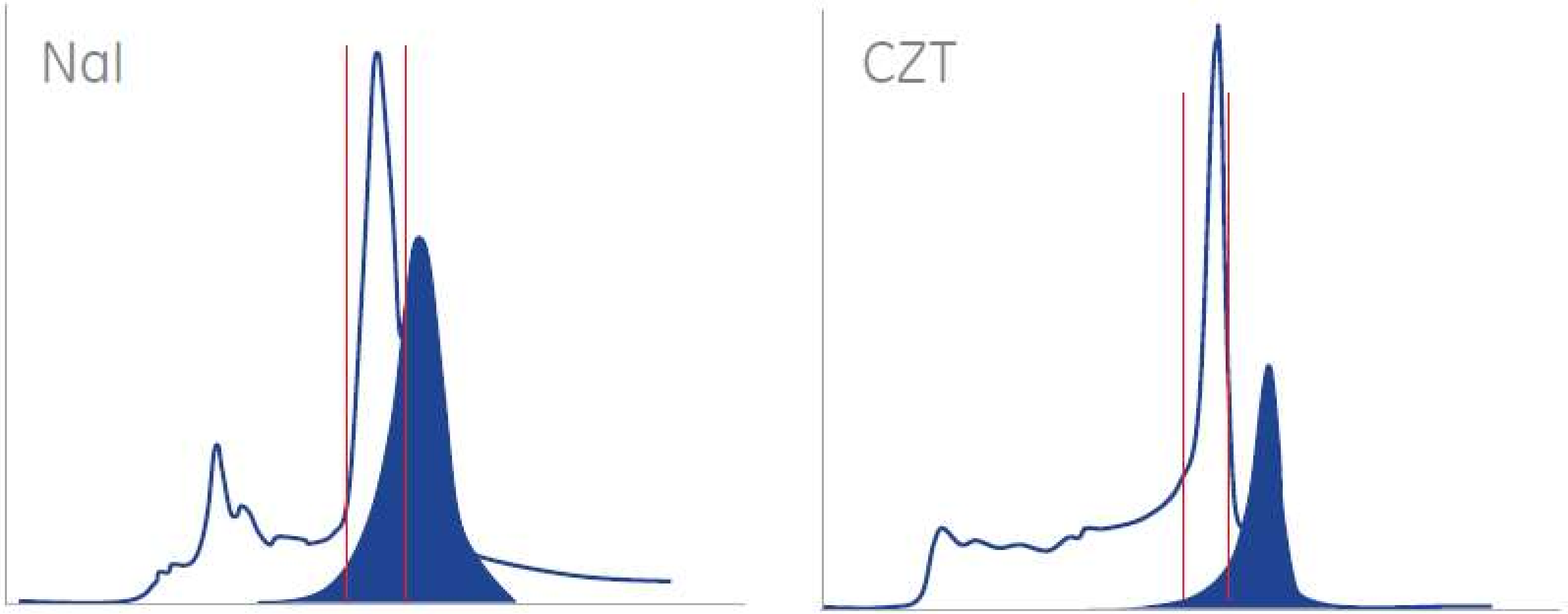

Overlay of ^{99m} Tc and ^{123}I spectra, showing greater crosstalk between the two peaks for the NaI detector with its poorer energy resolution and wider energy window.

CZT FWHM ~ 6 %, theoretical min1.5 %

NaI FWHM ~ 10 %, theoretical min 7 %

Cardiac Procedure

Conventional SPECT/CT

Discovery NM/CT 670 CZT

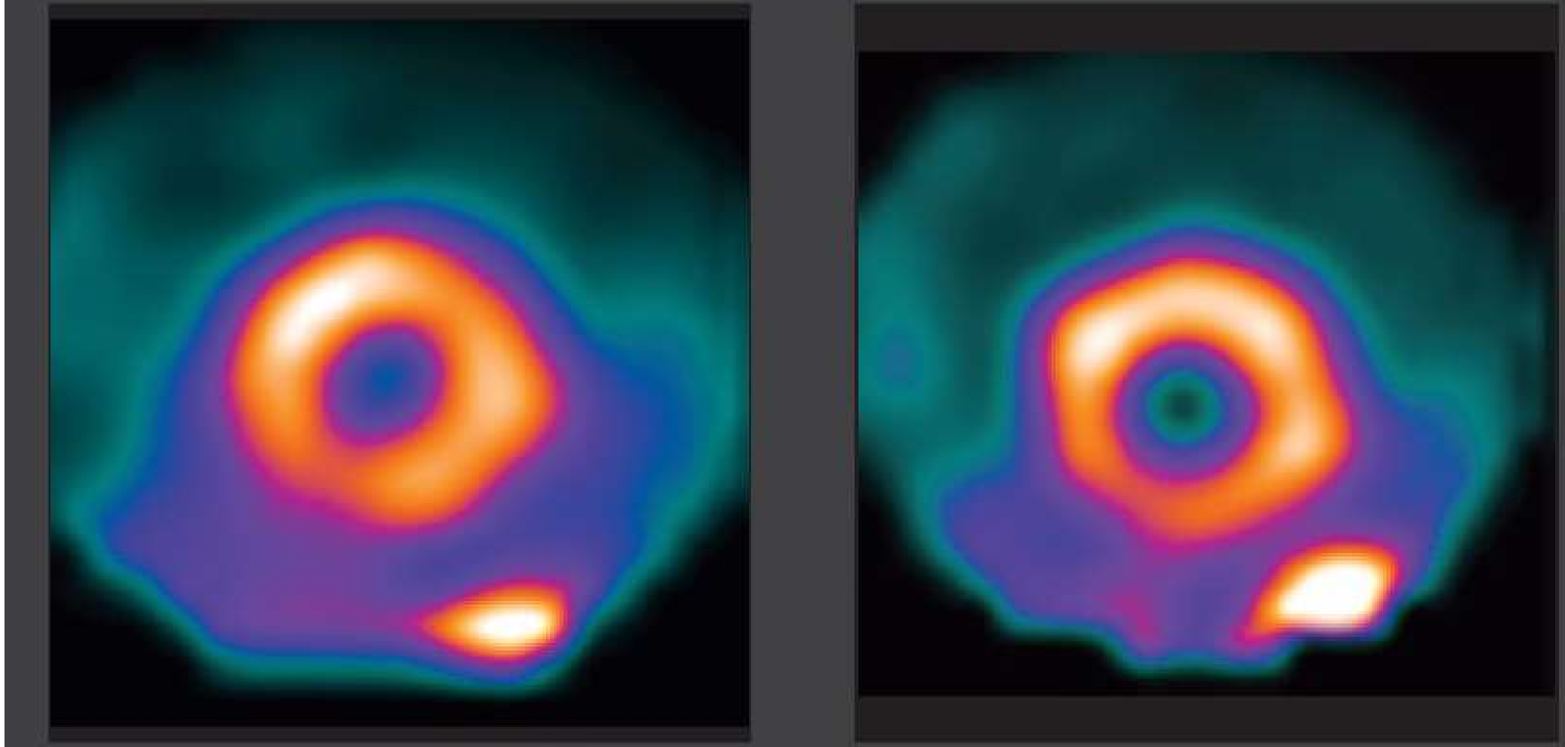

10 min

10 min

Positron Emission Tomography

β^+ Emission and Annihilation

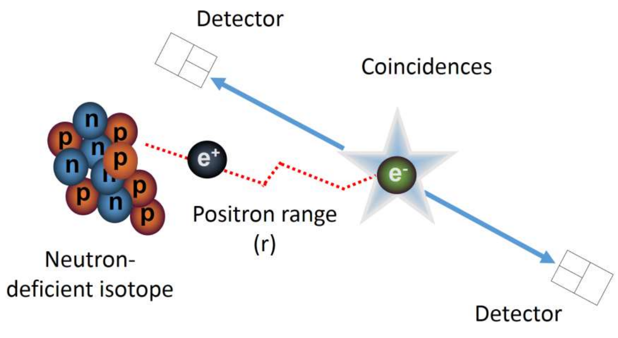

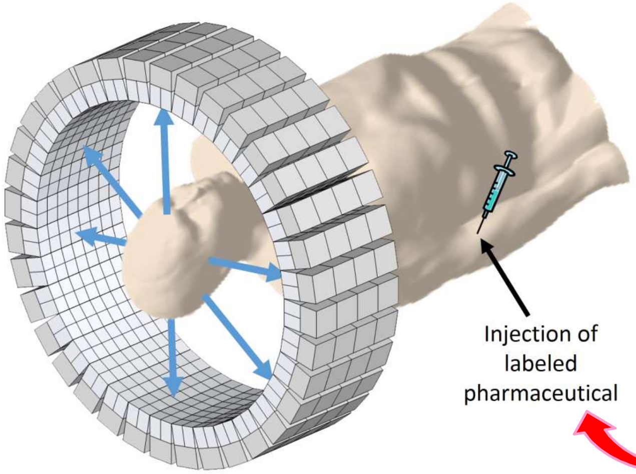

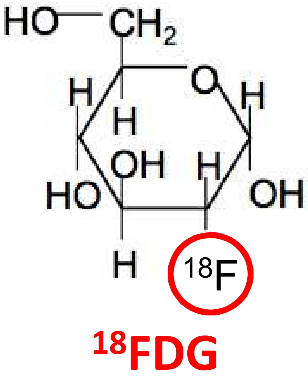

Parallel projections

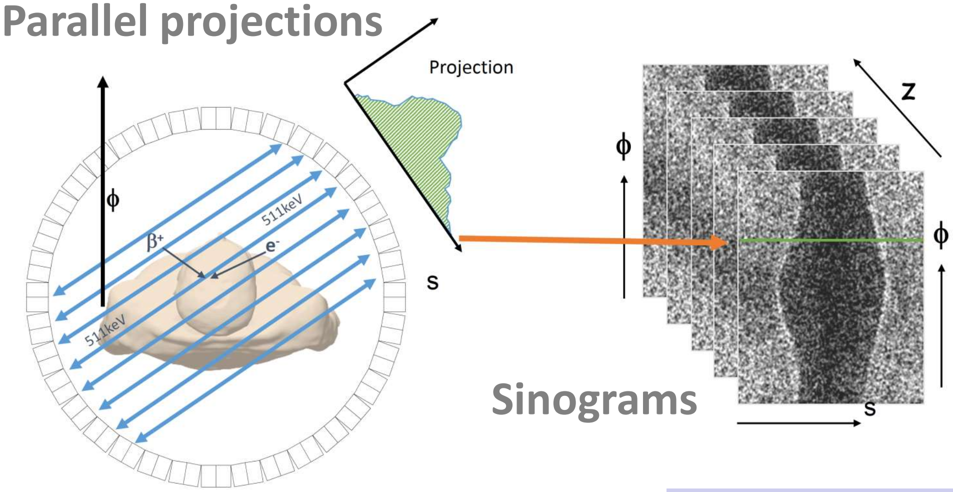

PET images

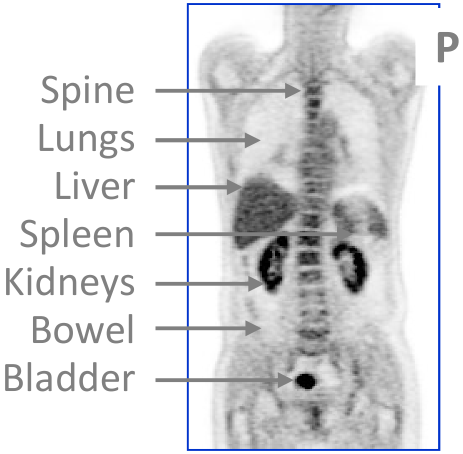

Modeling

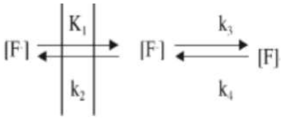

DW Townsend, Singapore

PET - detection

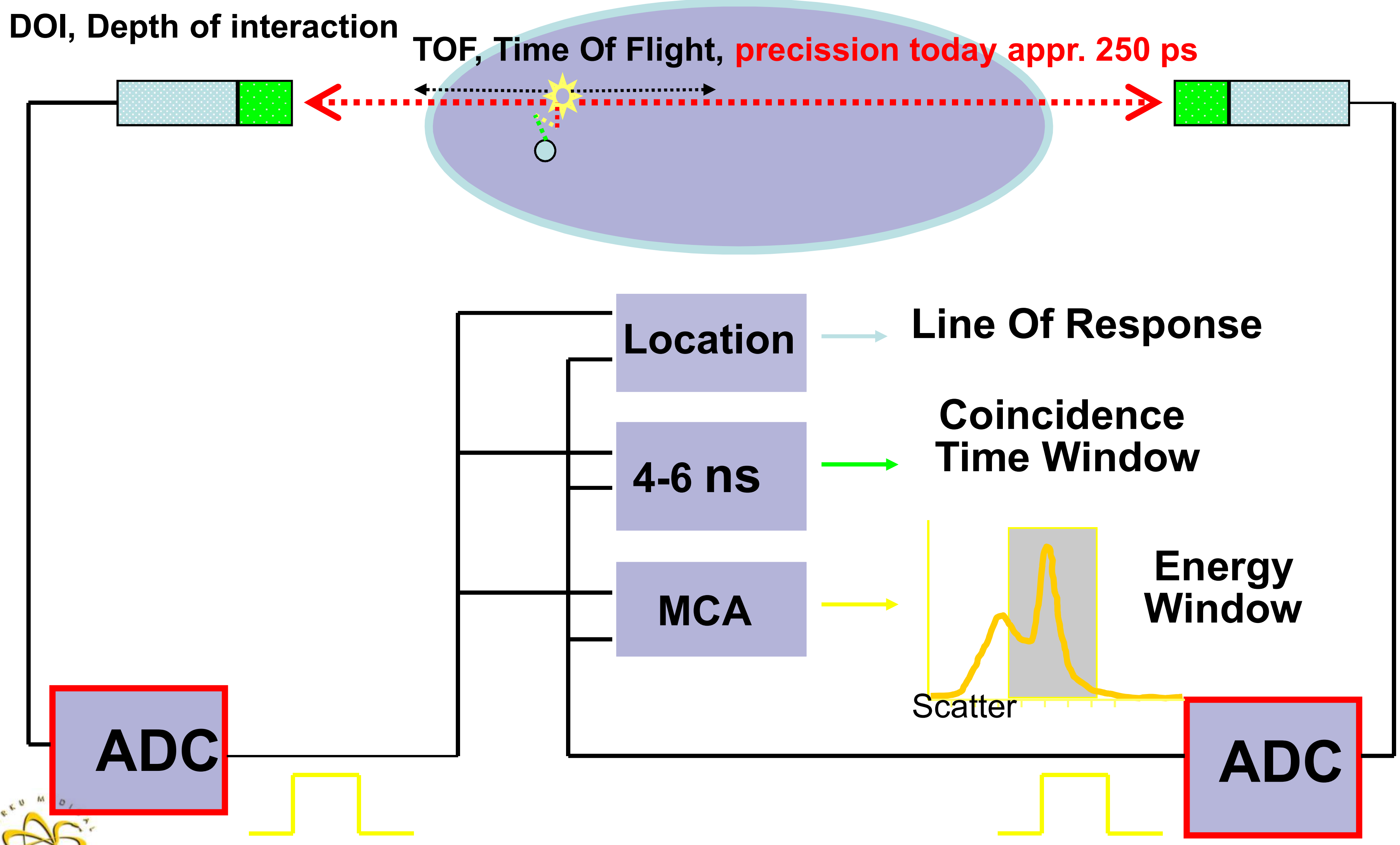

DOI, Depth of interaction

TOF, Time Of Flight, precission today appr. 250 ps

Location → **Line Of Response**

4-6 ns → **Coincidence Time Window**

MCA → **Energy Window**

Scatter

ADC

ADC

Spatial Resolution

$$\mathrm{FWHM} = a\sqrt{(d/2)^2 + b^2 + (0.0022D)^2 + r^2}$$

Reconstruction **Geometric** **Coding** **Non-Collinearity** **Positron Range**

Block Detectors

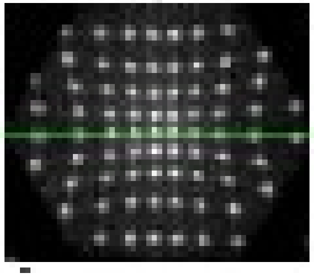

Panel Detectors

PMTs

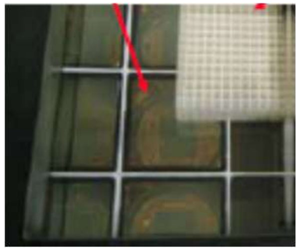

GE : DISCOVERY
BGO

CTI /SIEMENS
BIOGRAPH HiREZ
LSO

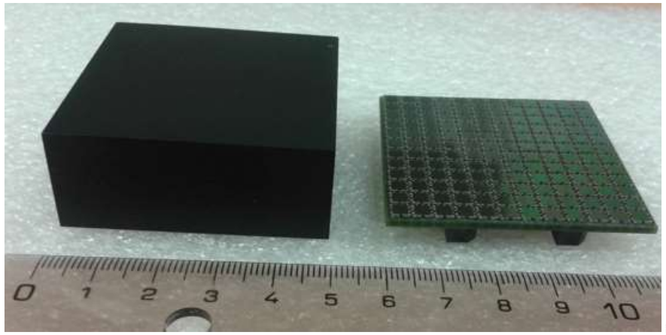

Monolite crystal (three 6 mm layers → DOI)
A 12 mm thick black painted trapezoidal (3x6mm) LYSO coupled to 12x12 standard SiPM-SensL array,
MindView brain insert

CTI / SIEMENS
LSO

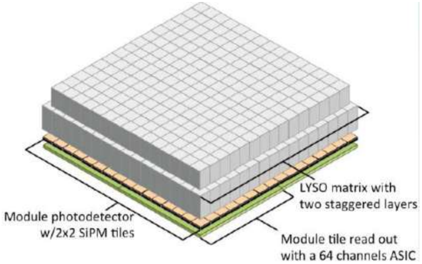

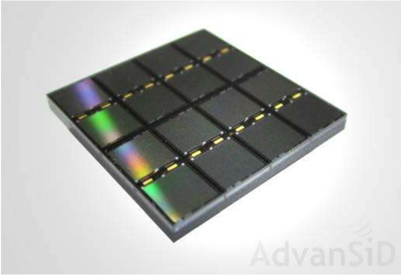

SiPM

b = 0 individual coupling

Partial Volume (PV) effect

effect of resolution and/or motion

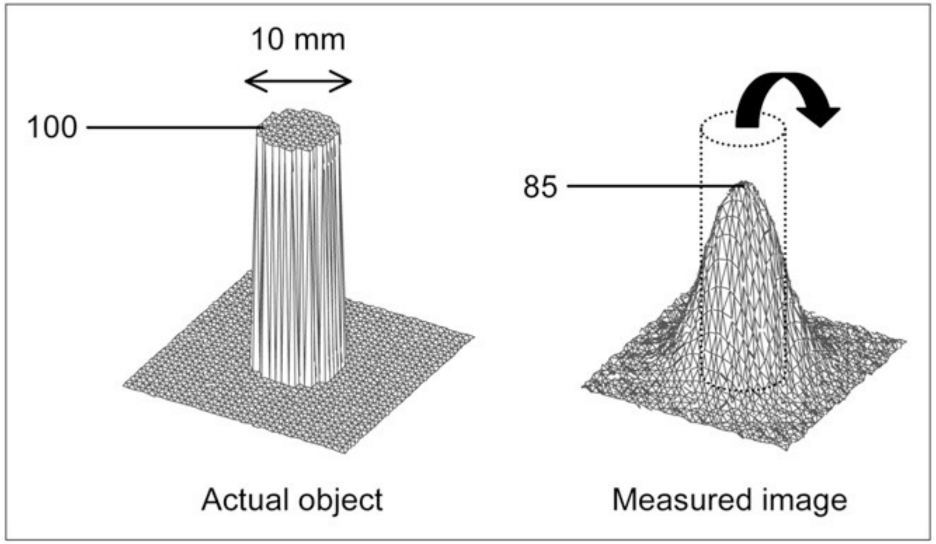

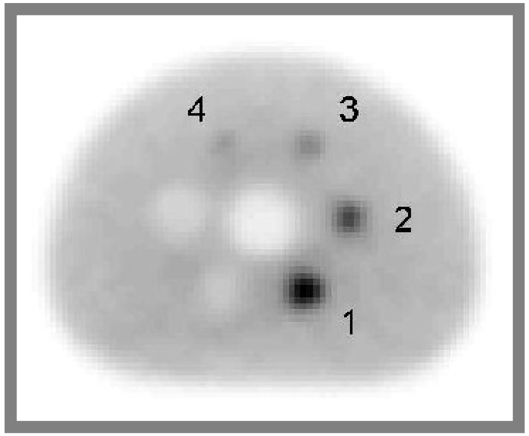

Approaches to PV correction

- iterative deconvolution (subject to noise)
- account for known anatomy (from MRI)
  - introduce an anatomical prior during reconstruction
  - apply correction based on anatomy post-reconstruction

Soret et al. JNM, 48:932-945, 2007
Erlandsson et al. Phys Med Biol 2012; 57: R119

Time Of Flight PET

TOF information can be used in the Reconstruction of the PET data to constraint the possible locations of the annihilation site along the line

Reconstruction without TOF information assumes that all the possible locations of the annihilation site along the line are equally likely.

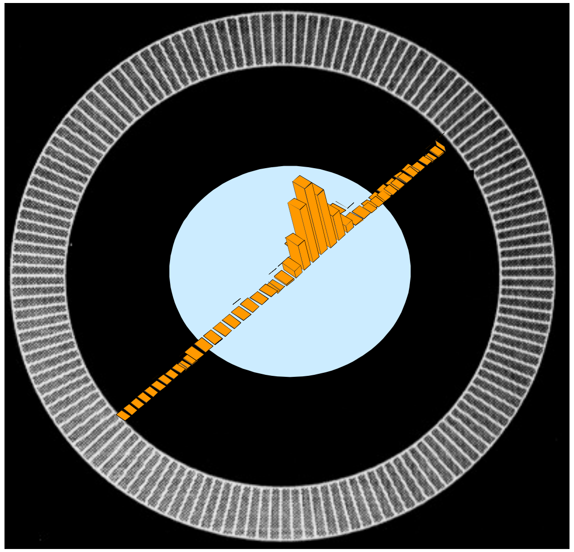

TOF

$$\Delta x = \frac{c\,\Delta t}{2}$$

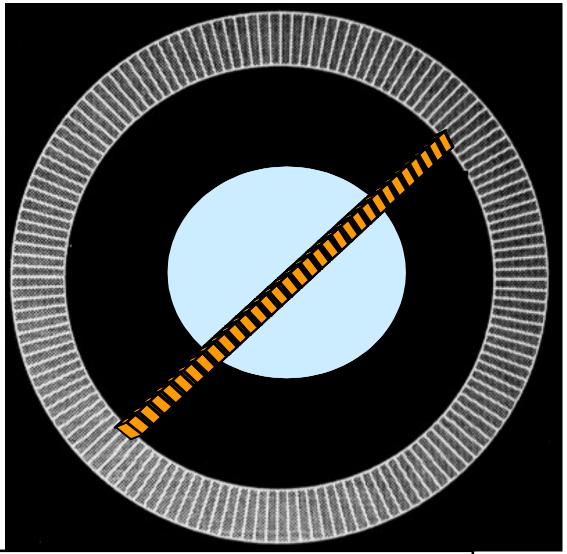

NON TOF

	Line	SNR GAIN	
Δt psec	Δx mm	D=20 cm	D=35 cm
50	0.75	5.2	6.8
300	4.5	2.1	2.8
500	7.5	1.6	2.2
650	9.75	1.4	1.9

$$\frac{SNR_{TOF}}{SNR} = \sqrt{\frac{2\,D}{c\,\Delta t}} = \sqrt{\frac{D}{\Delta x}}$$

Depth Of Interaction, DOI

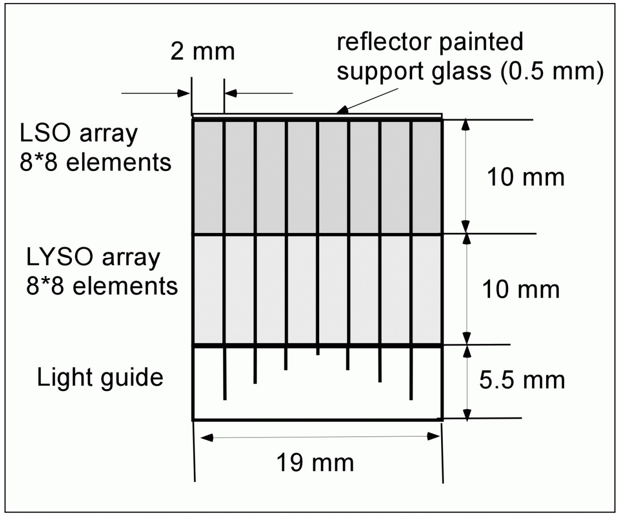

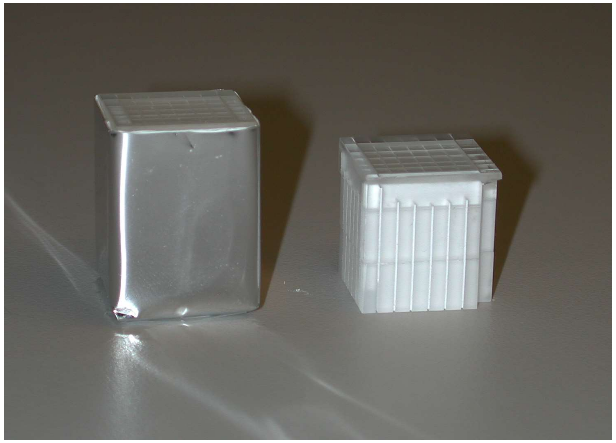

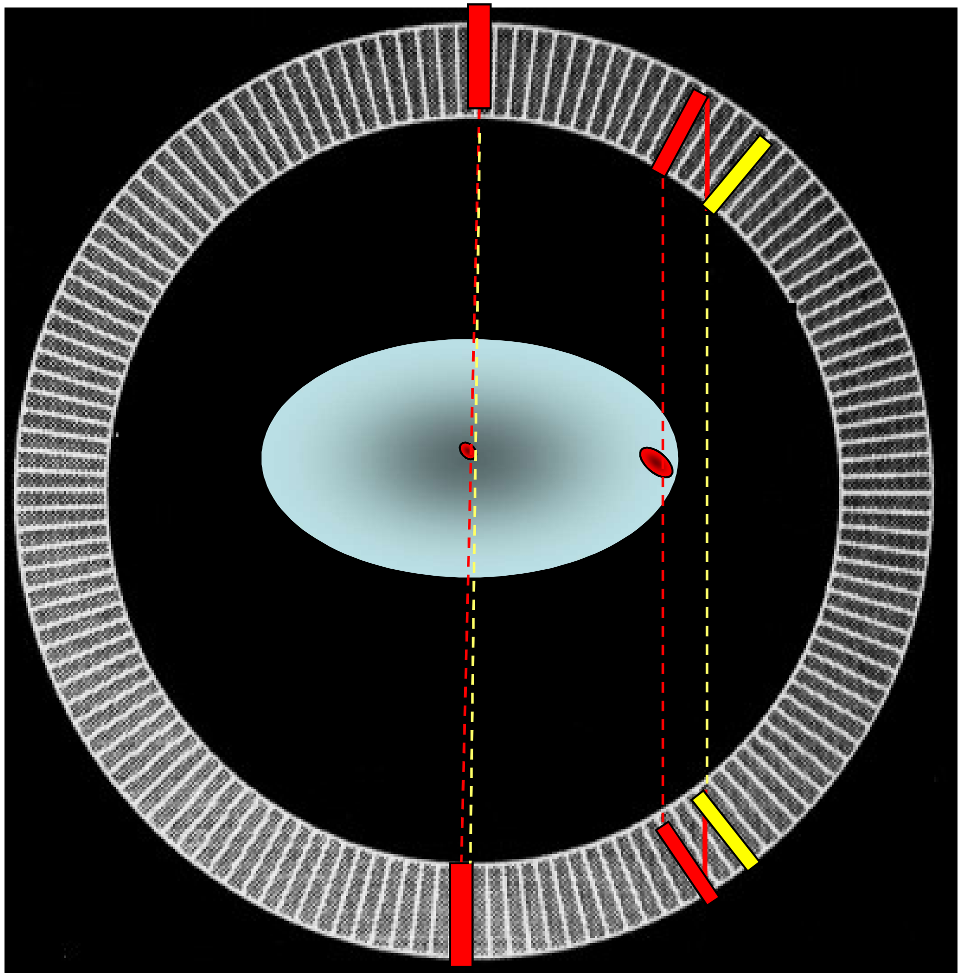

- Bore diameter
- Crystal length

Spatial resolution
degrades towards edges

PET/CT or PET/MR?

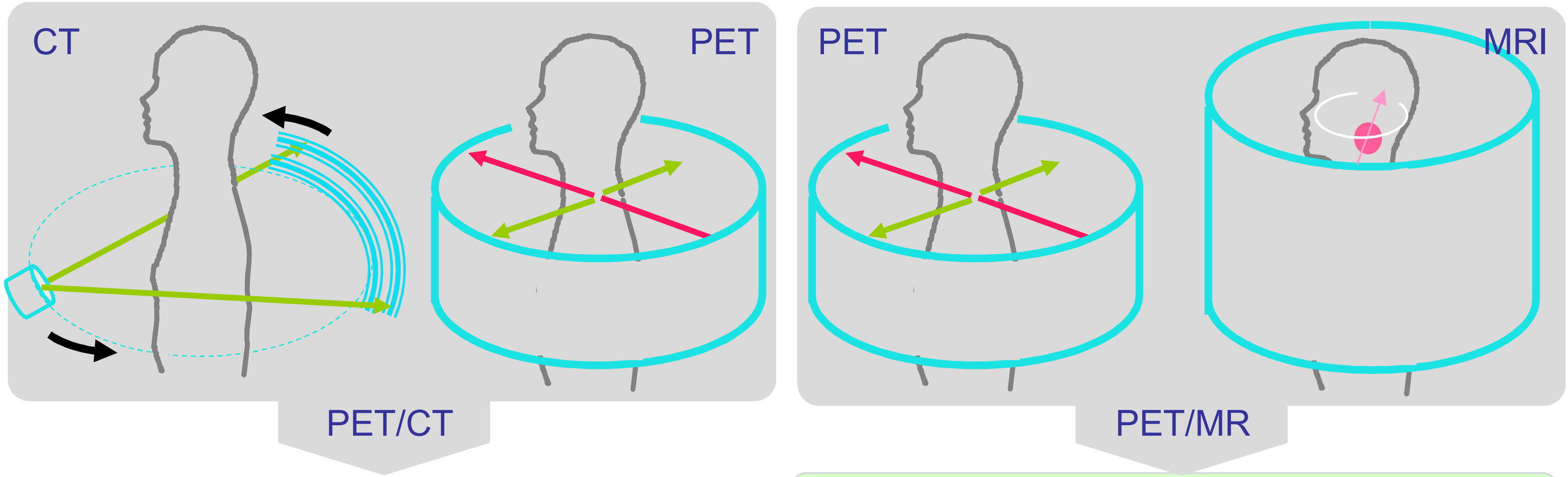

pro

High-resolution anatomy

Best possible, **intrinsic co-registration**

Accurate attenuation correction

Fast whole-body imaging

High **soft tissue contrast**

Oblique image planes (“**no-dose tilt**”)

Quasi-simultaneous imaging

Less radiation dose (MR = 0)

con

Patient exposure from CT

Motion-induced misalignment

Not simultaneous

MR-compatible PET detector

MR-based attenuation correction

Clinical and research **applications**

Limited sensitivity for pulmonary lesions

Modified from T Bayer

Respiratory motion: 4D PET/CT

When scanner resolution and correction algorithms get better

Errors from breathing motion is to be corrected.

Difference in the acquisition time in CT and PET.

CT in breath hold and PET in free breathing

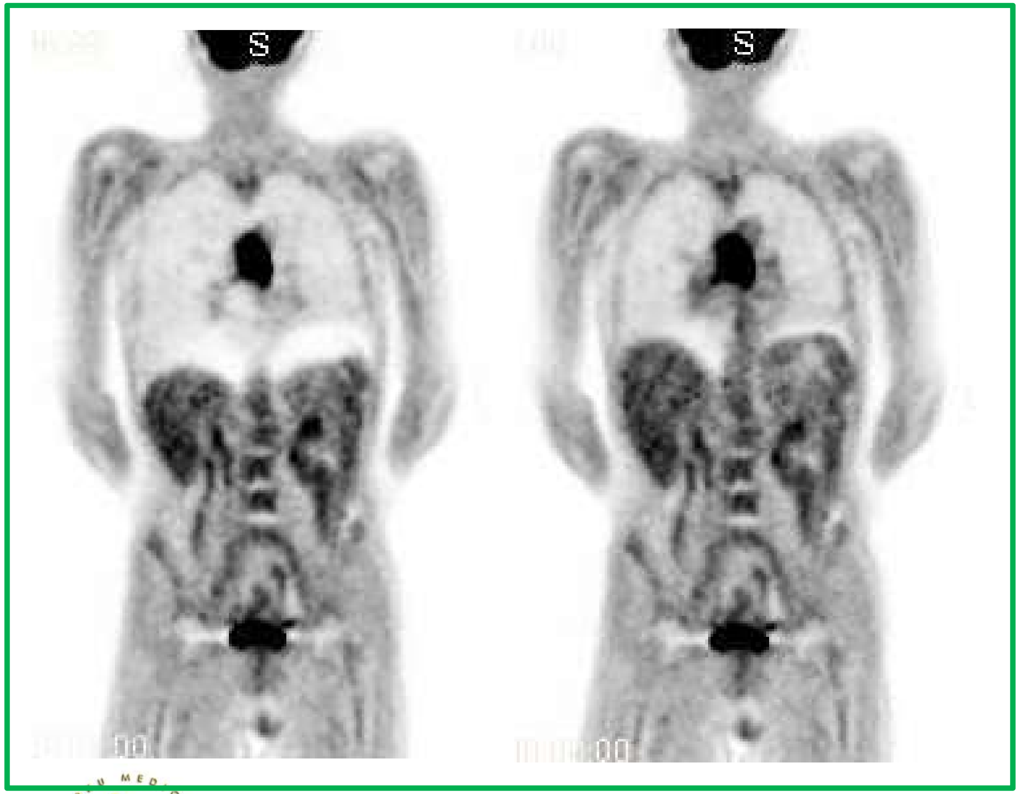

D Visvikis, et al; Eur J Nucl Med 2003, 30(3), 344-353

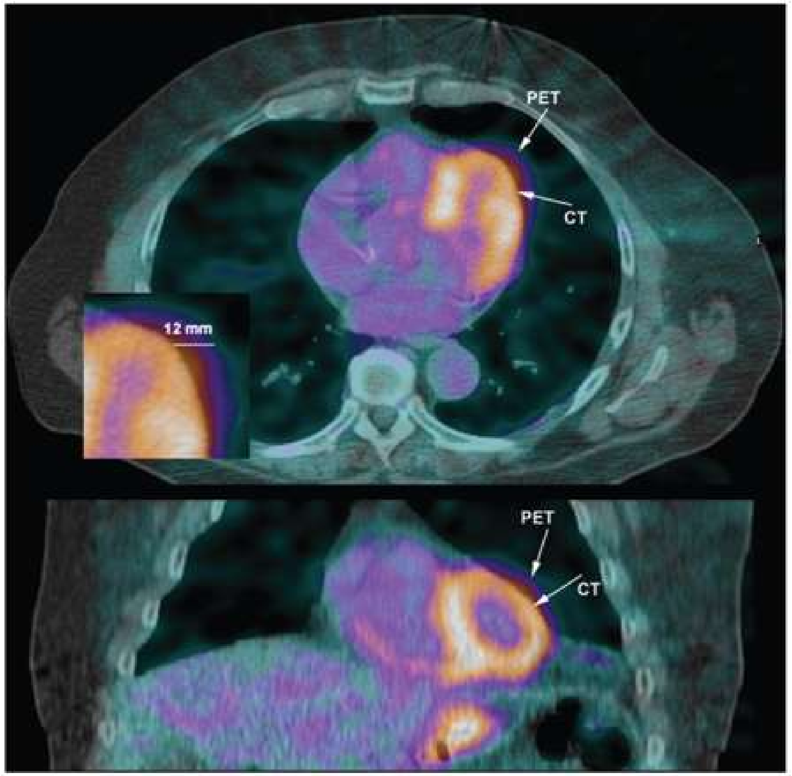

K Lance Gould, et al; J Nucl Med 2007, 48, 1112-1121

RPM Respiratory Gating™ System

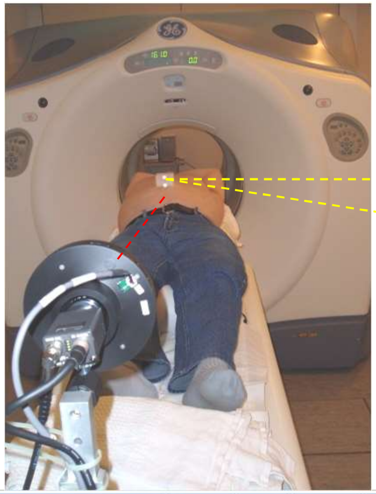

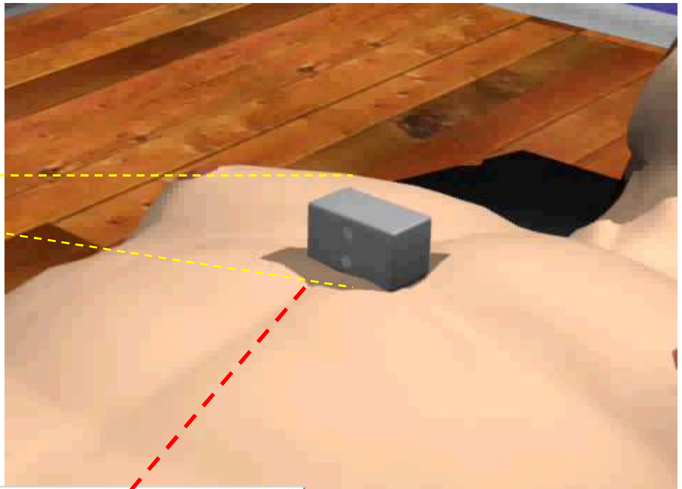

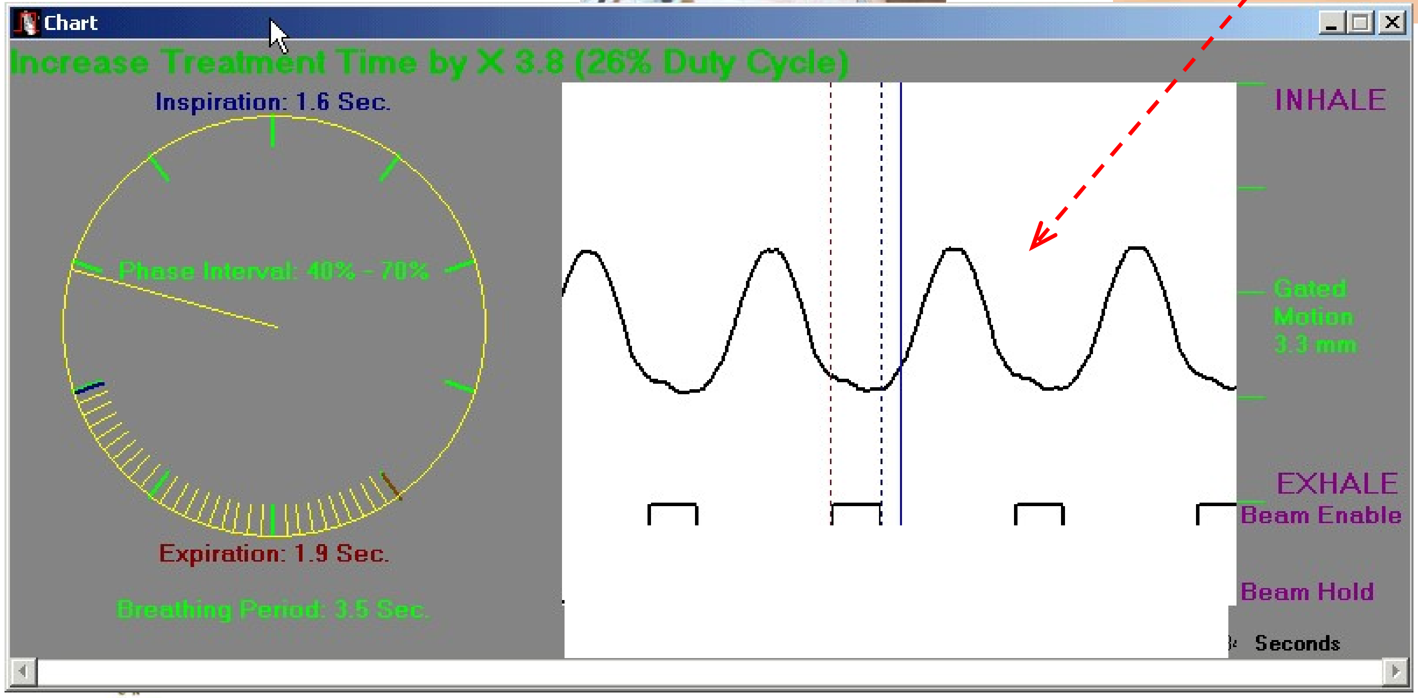

Increase Treatment Time by X 3.8 (26% Duty Cycle)

Inspiration: 1.6 Sec.

Phase Interval: 40% - 70%

Expiration: 1.9 Sec.

Breathing Period: 3.5 Sec.

TM : Varian Medical System
Gating School Copenhagen

PET/CT systems with 4D → Lesion Detectability

Conventional PET/CT systems with
Static acquisitions

PET/CT Systems with **4D**
Respiratory Gating

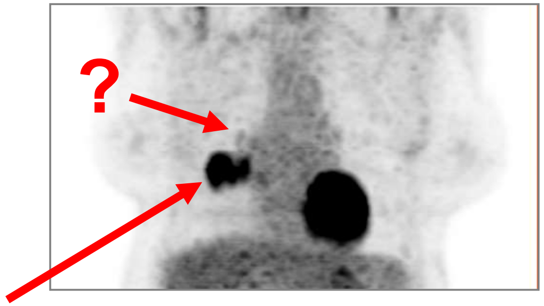

Primary Tumor

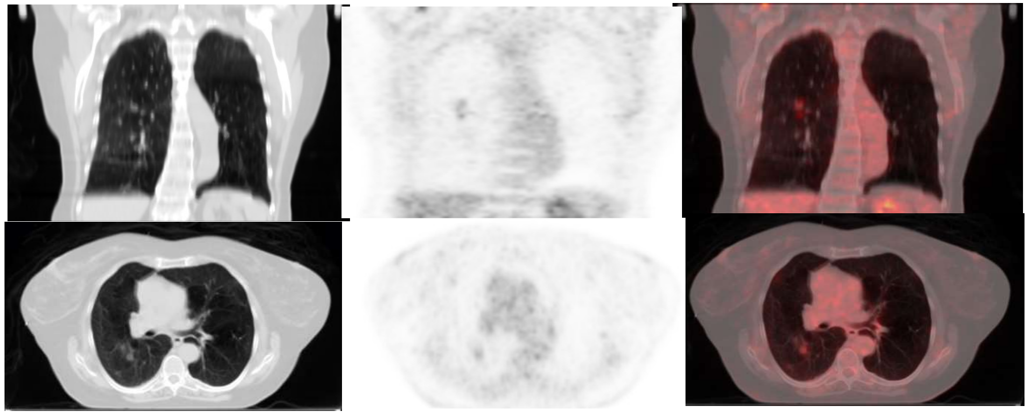

Questionable on CT and appears like normal tissue (same activity) ?

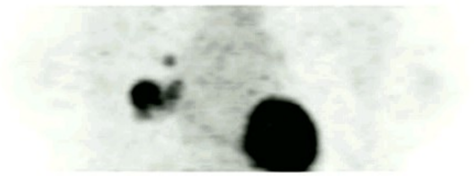

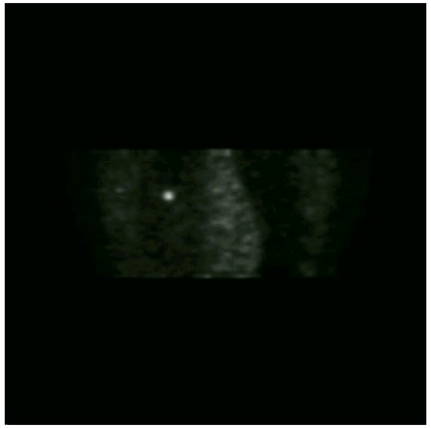

Courtesy of Holyname Hospital

Images courtesy of Holy Name Hospital

MoCo from Static CT and gated PET

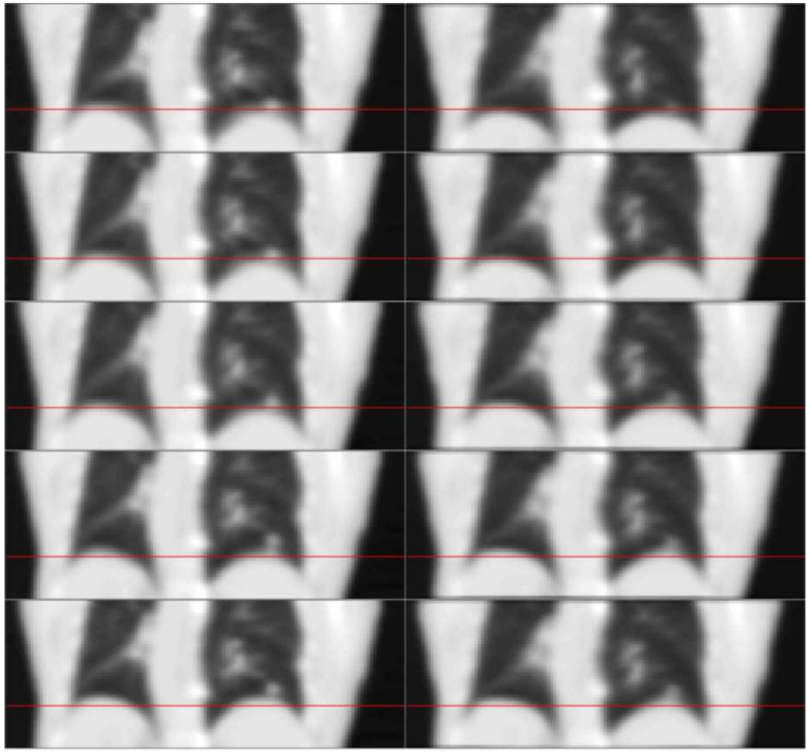

(a) (b)

Gated CT JRM-Wrap CT

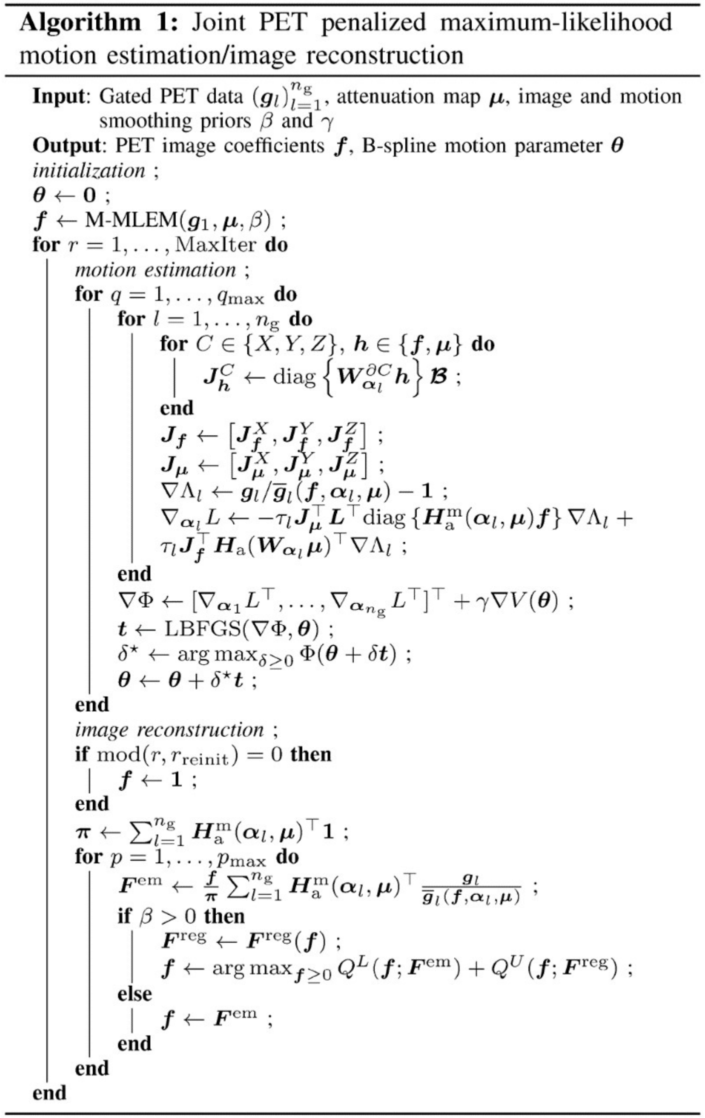

Algorithm 1: Joint PET penalized maximum-likelihood motion estimation/image reconstruction

```
Input: Gated PET data $(\boldsymbol{g}_l)_{l=1}^{n_\mathrm{g}}$, attenuation map $\boldsymbol{\mu}$, image and motion
       smoothing priors $\beta$ and $\gamma$
Output: PET image coefficients $\boldsymbol{f}$, B-spline motion parameter $\boldsymbol{\theta}$
initialization ;
$\boldsymbol{\theta} \leftarrow \mathbf{0}$ ;
$\boldsymbol{f} \leftarrow \text{M-MLEM}(\boldsymbol{g}_1, \boldsymbol{\mu}, \beta)$ ;
for $r = 1, \ldots, \mathrm{MaxIter}$ do
    motion estimation ;
    for $q = 1, \ldots, q_{\max}$ do
        for $l = 1, \ldots, n_\mathrm{g}$ do
            for $C \in \{X, Y, Z\}$, $\boldsymbol{h} \in \{\boldsymbol{f}, \boldsymbol{\mu}\}$ do
                $\boldsymbol{J}_{\boldsymbol{h}}^{C} \leftarrow \mathrm{diag}\left\{\boldsymbol{W}_{\boldsymbol{\alpha}_l}^{\partial C} \boldsymbol{h}\right\} \boldsymbol{\mathcal{B}}$ ;
            end
            $\boldsymbol{J}_{\boldsymbol{f}} \leftarrow \left[\boldsymbol{J}_{\boldsymbol{f}}^{X}, \boldsymbol{J}_{\boldsymbol{f}}^{Y}, \boldsymbol{J}_{\boldsymbol{f}}^{Z}\right]$ ;
            $\boldsymbol{J}_{\boldsymbol{\mu}} \leftarrow \left[\boldsymbol{J}_{\boldsymbol{\mu}}^{X}, \boldsymbol{J}_{\boldsymbol{\mu}}^{Y}, \boldsymbol{J}_{\boldsymbol{\mu}}^{Z}\right]$ ;
            $\nabla \Lambda_l \leftarrow \boldsymbol{g}_l / \overline{\boldsymbol{g}}_l(\boldsymbol{f}, \boldsymbol{\alpha}_l, \boldsymbol{\mu}) - \mathbf{1}$ ;
            $\nabla_{\boldsymbol{\alpha}_l} L \leftarrow -\tau_l \boldsymbol{J}_{\boldsymbol{\mu}}^{\top} \boldsymbol{L}^{\top} \mathrm{diag}\left\{\boldsymbol{H}_\mathrm{a}^\mathrm{m}(\boldsymbol{\alpha}_l, \boldsymbol{\mu}) \boldsymbol{f}\right\} \nabla \Lambda_l +$
            $\tau_l \boldsymbol{J}_{\boldsymbol{f}}^{\top} \boldsymbol{H}_\mathrm{a}(\boldsymbol{W}_{\boldsymbol{\alpha}_l} \boldsymbol{\mu})^{\top} \nabla \Lambda_l$ ;
        end
        $\nabla \Phi \leftarrow [\nabla_{\boldsymbol{\alpha}_1} L^{\top}, \ldots, \nabla_{\boldsymbol{\alpha}_{n_\mathrm{g}}} L^{\top}]^{\top} + \gamma \nabla V(\boldsymbol{\theta})$ ;
        $\boldsymbol{t} \leftarrow \mathrm{LBFGS}(\nabla \Phi, \boldsymbol{\theta})$ ;
        $\delta^{\star} \leftarrow \arg\max_{\delta \geq 0} \Phi(\boldsymbol{\theta} + \delta \boldsymbol{t})$ ;
        $\boldsymbol{\theta} \leftarrow \boldsymbol{\theta} + \delta^{\star} \boldsymbol{t}$ ;
    end
    image reconstruction ;
    if $\mathrm{mod}(r, r_\mathrm{reinit}) = 0$ then
        $\boldsymbol{f} \leftarrow \mathbf{1}$ ;
    end
    $\boldsymbol{\pi} \leftarrow \sum_{l=1}^{n_\mathrm{g}} \boldsymbol{H}_\mathrm{a}^\mathrm{m}(\boldsymbol{\alpha}_l, \boldsymbol{\mu})^{\top} \mathbf{1}$ ;
    for $p = 1, \ldots, p_{\max}$ do
        $\boldsymbol{F}^\mathrm{em} \leftarrow \frac{\boldsymbol{f}}{\boldsymbol{\pi}} \sum_{l=1}^{n_\mathrm{g}} \boldsymbol{H}_\mathrm{a}^\mathrm{m}(\boldsymbol{\alpha}_l, \boldsymbol{\mu})^{\top} \frac{\boldsymbol{g}_l}{\overline{\boldsymbol{g}}_l(\boldsymbol{f}, \boldsymbol{\alpha}_l, \boldsymbol{\mu})}$ ;
        if $\beta > 0$ then
            $\boldsymbol{F}^\mathrm{reg} \leftarrow \boldsymbol{F}^\mathrm{reg}(\boldsymbol{f})$ ;
            $\boldsymbol{f} \leftarrow \arg\max_{\boldsymbol{f} \geq 0} Q^{L}(\boldsymbol{f}; \boldsymbol{F}^\mathrm{em}) + Q^{U}(\boldsymbol{f}; \boldsymbol{F}^\mathrm{reg})$ ;
        else
            $\boldsymbol{f} \leftarrow \boldsymbol{F}^\mathrm{em}$ ;
        end
    end
end
```

Maximum-Likelihood Joint Image Reconstruction/Motion Estimation in Attenuation-Corrected Respiratory Gated PET/CT Using a Single Attenuation Map

Alexandre Bousse, Ottavia Bertolli, David Atkinson, Simon Arridge, Sébastien Ourselin, Brian F. Hutton*, Senior Member, IEEE*, and Kris Thielemans*, Senior Member, IEEE*m

IEEE TRANSACTIONS ON MEDICAL IMAGING, VOL. 35, NO. 1, JANUARY 2016

Next step: motion correction

Q Freeze

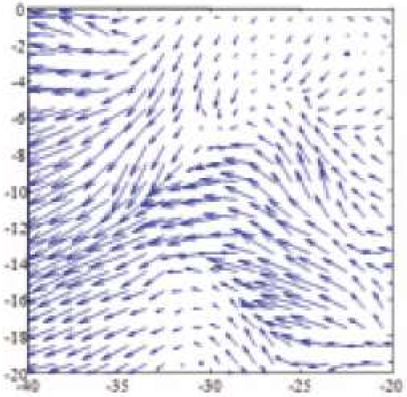

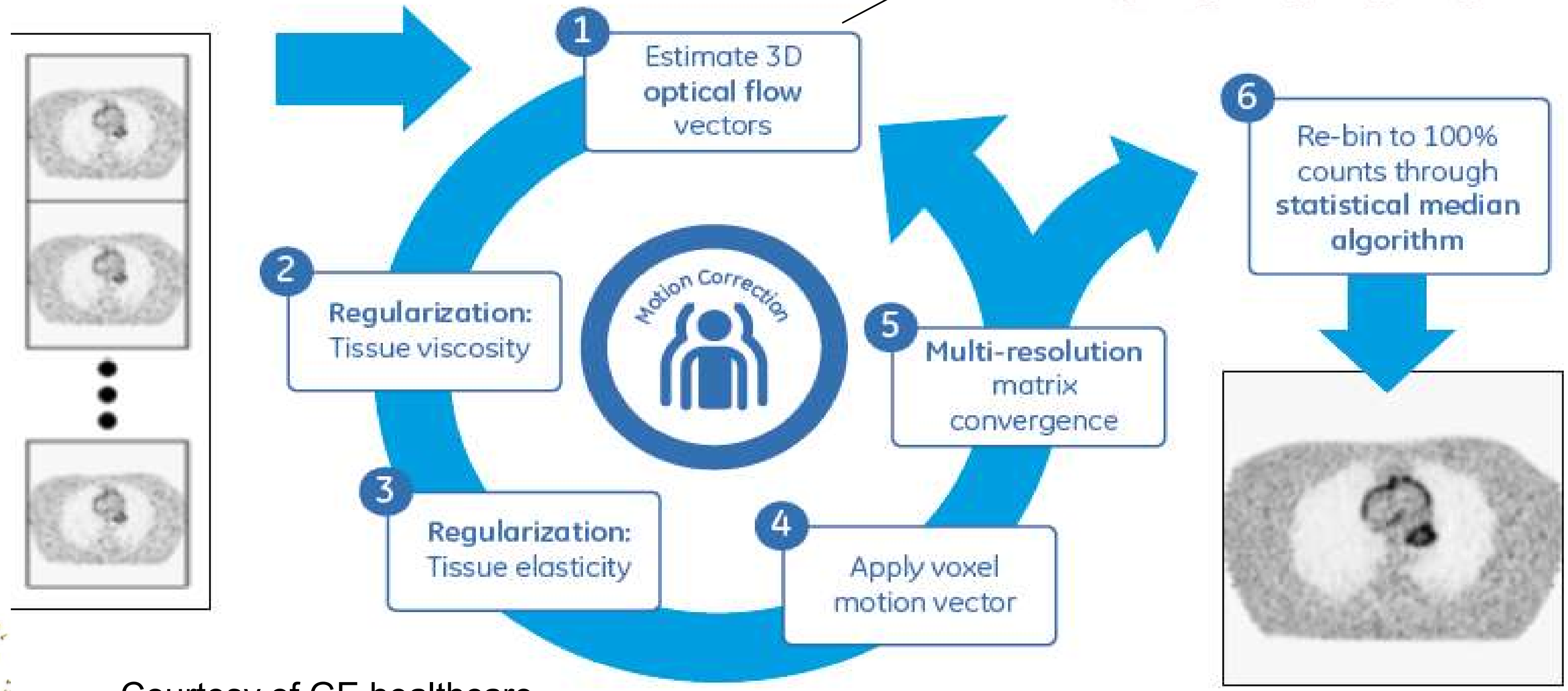

1 Estimate 3D **optical flow** vectors

2 **Regularization:** Tissue viscosity

3 **Regularization:** Tissue elasticity

4 Apply voxel motion vector

5 **Multi-resolution** matrix convergence

6 Re-bin to 100% counts through **statistical median algorithm**

Courtesy of GE healthcare

Example of MoCo

- improved lesion detection and localisation
- artefact reduction
- improved quantification

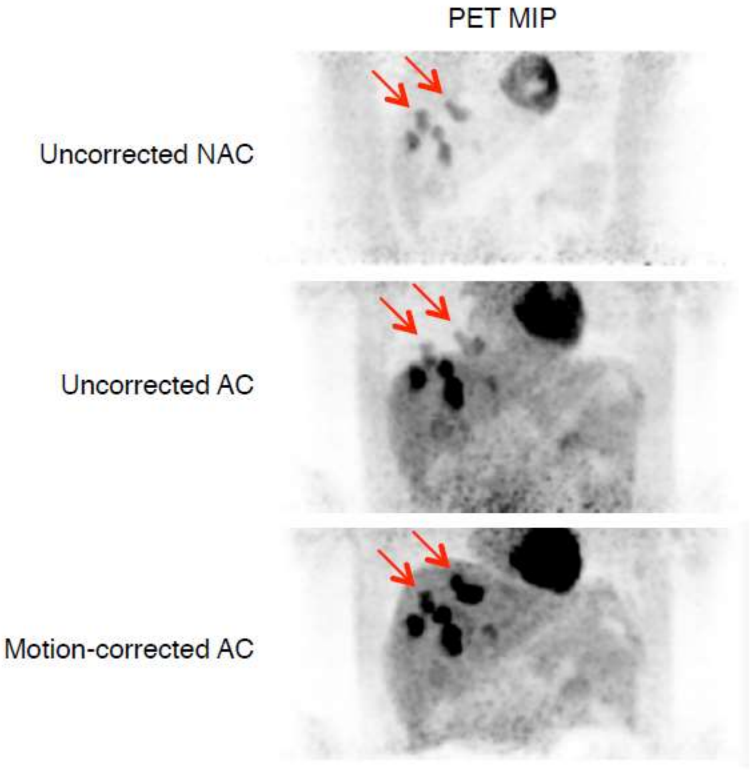

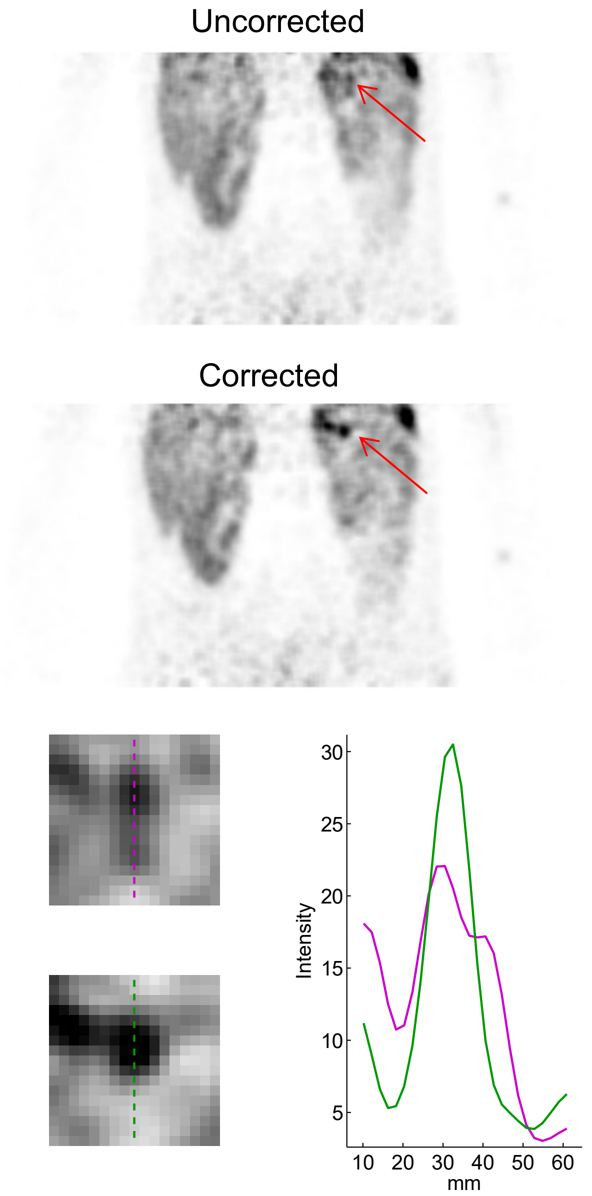

Manber et al. J Nucl Med 2015; 56: 890.
Manber et al. Phys Med Biol 2016; 61: 6515

CT vs MR in Image Segmentation

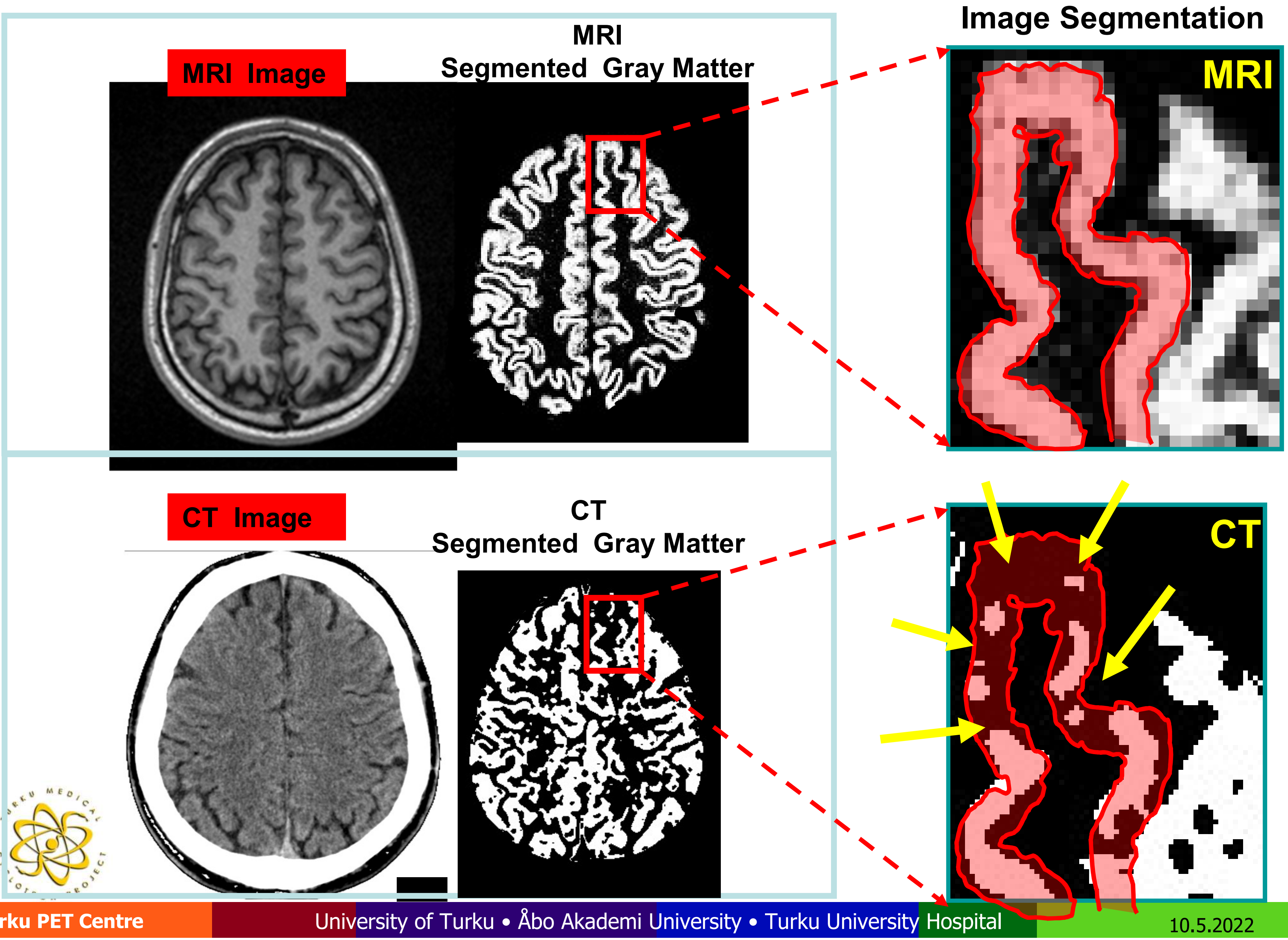

MRI Image

MRI
Segmented Gray Matter

CT Image

CT
Segmented Gray Matter

Image Segmentation

MRI

CT

PMT is sensitive to magnetic fields

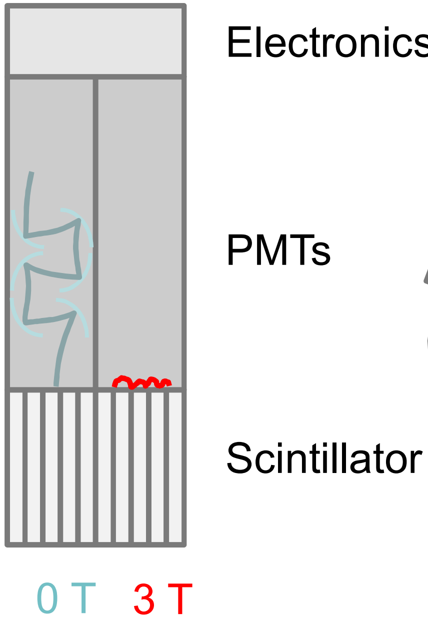

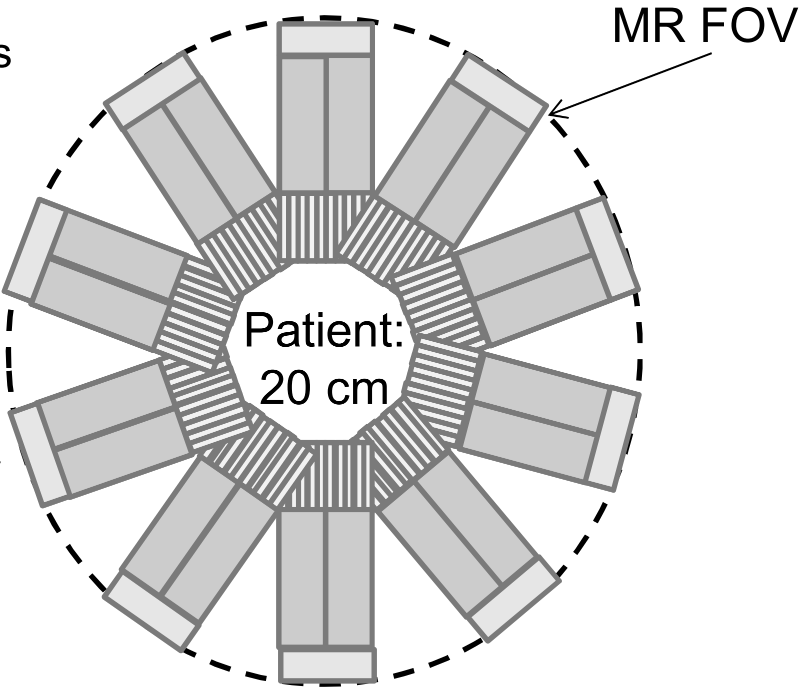

- A conventional PET detector leaves insufficient space for the patient

Replace PMT with SiPM based detector

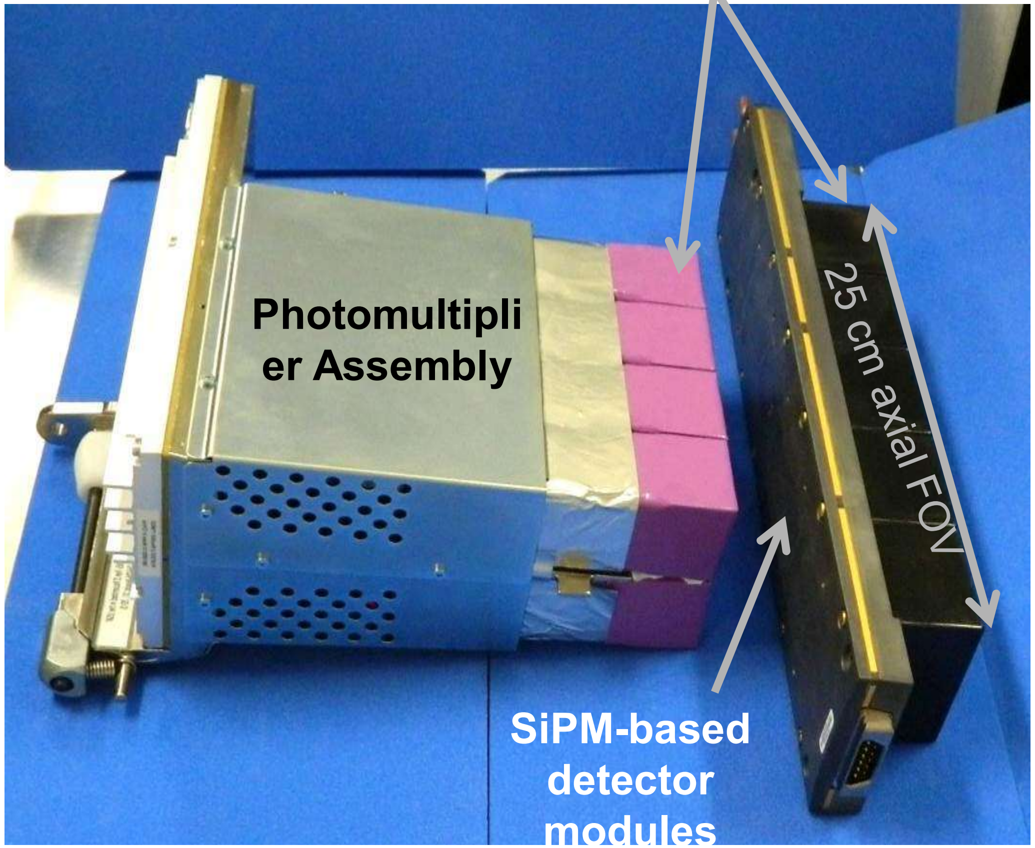

25 mm crystals

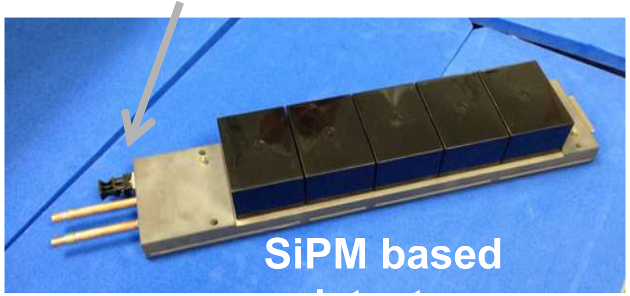

Optical fiber output

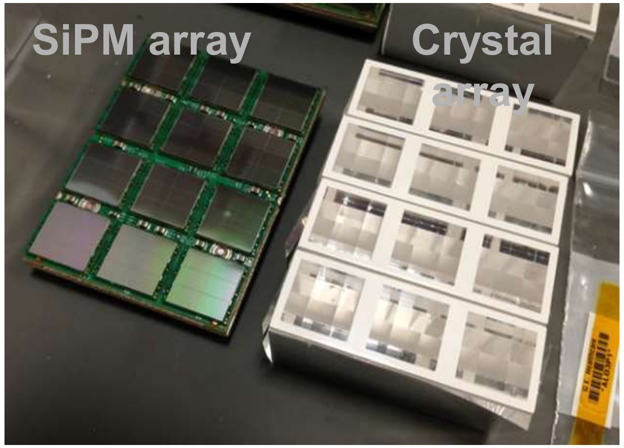

PET/MR: Challenges and Solutions

PET/MR system design (fromThomas Beyer)

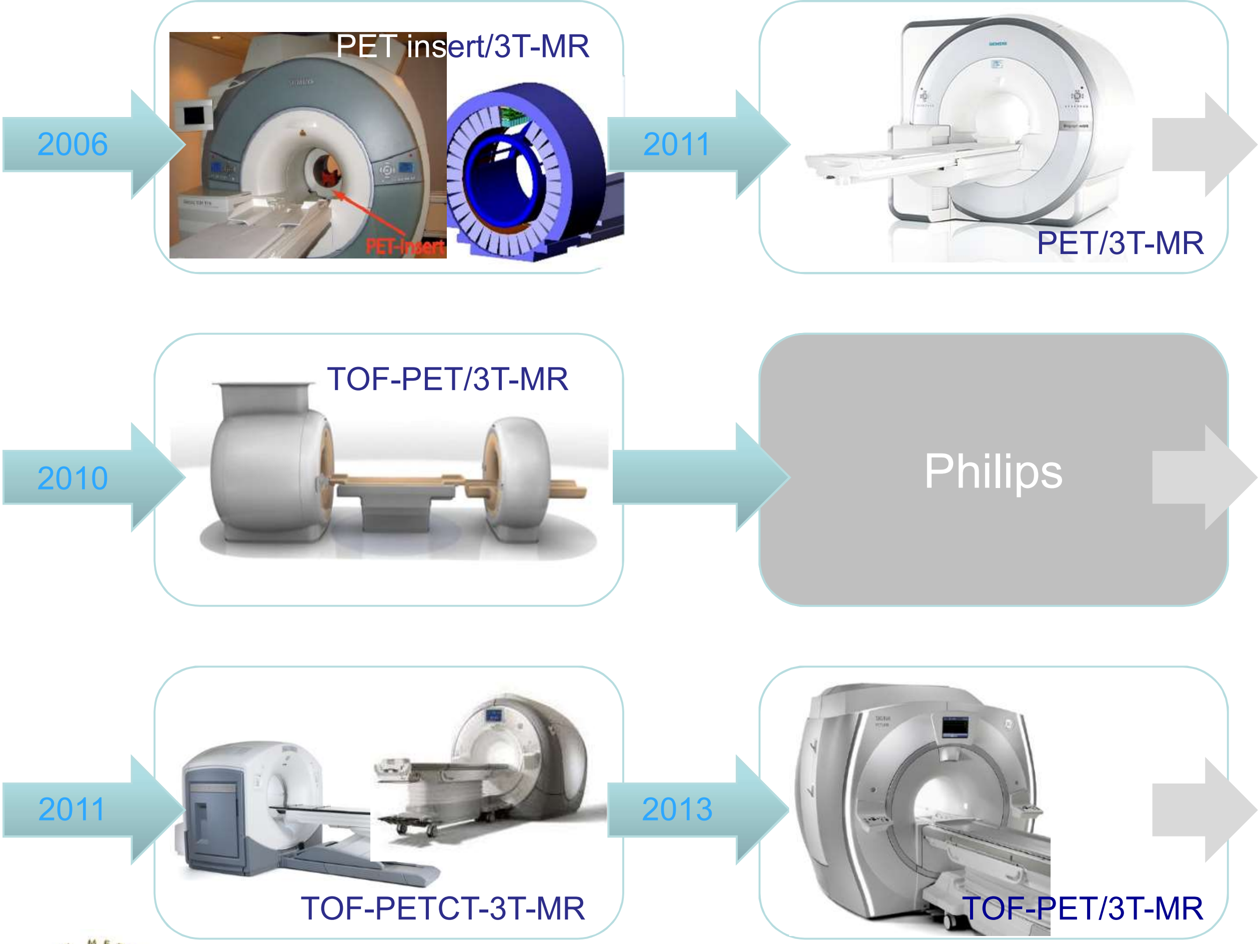

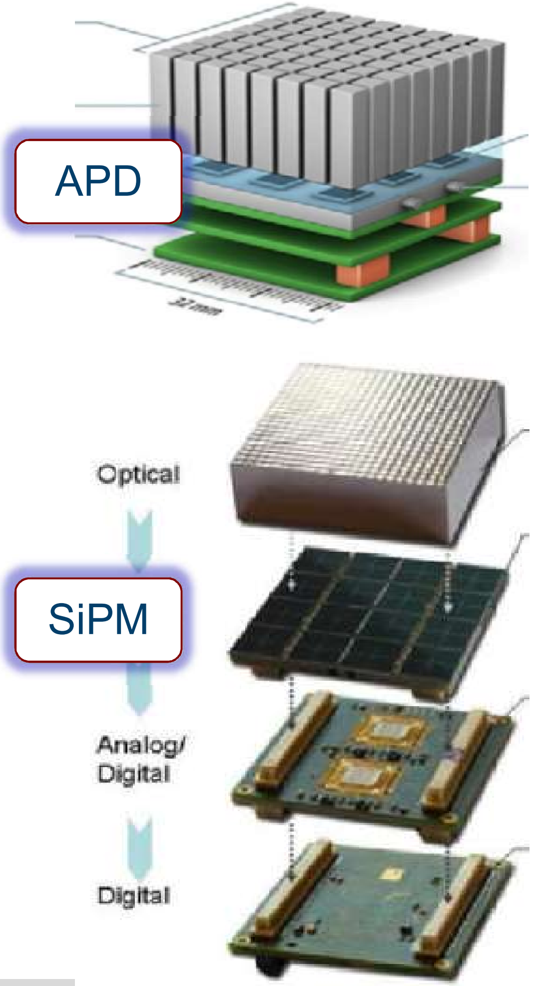

System integration driven by progressive technology.

GE Signa PET/MR

https://www.gehealthcare.com/products/magnetic-resonance-imaging/3-0t/signa-pet-mr

January 2020
Image Virva Saunavaara

Installation

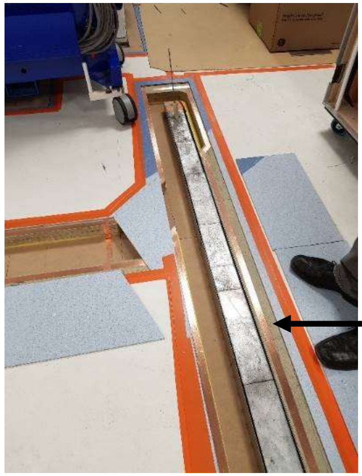

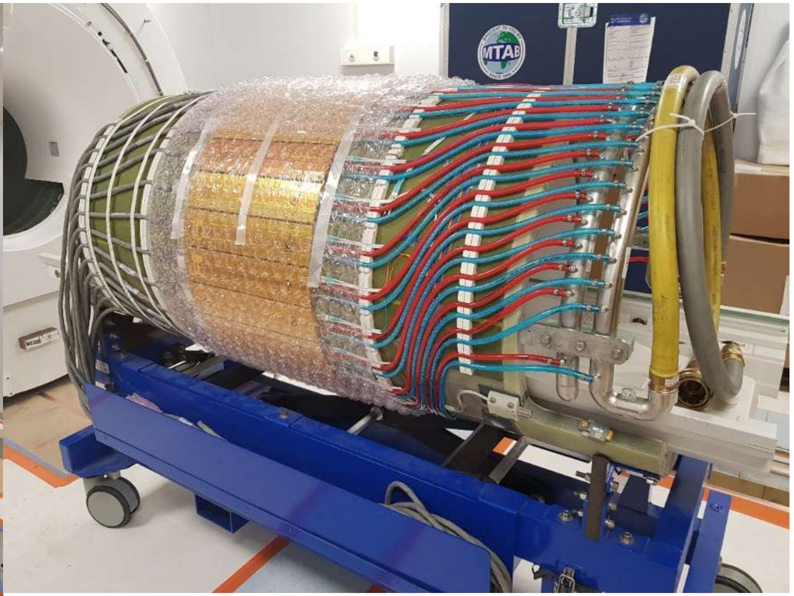

O-15 gas rails MR gantry PET Insert.

Photos:Virva Saunavaara

FUTURE of MMMI

PET 20.0: a cost-efficient, 2mm spatial resolution Total Body PET with point sensitivity up to 22% and adaptive axial FOV of maximum 2.00m

__S. Vandenberghe__, E. Mikhalyova, B. Brans, M. Defrise, T. Lahoutte, K. Muylle, R. Van Hole, D. R. Schaart, J. S. Karp; Gent, UC Davies, Delft, U PENN

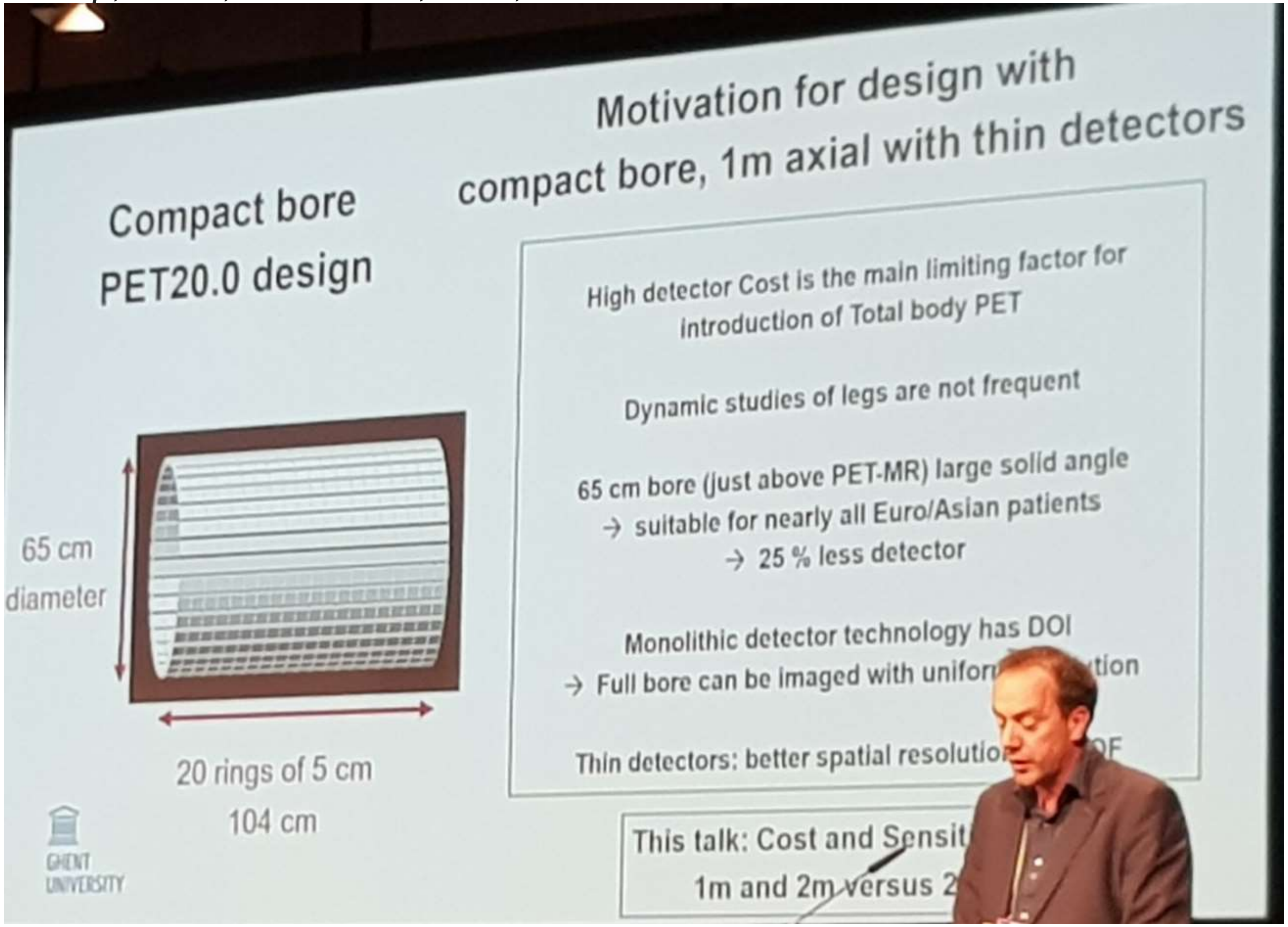

Motivation for design with
compact bore, 1m axial with thin detectors

Compact bore
PET20.0 design

65 cm
diameter

20 rings of 5 cm
104 cm

GHENT
UNIVERSITY

High detector Cost is the main limiting factor for
introduction of Total body PET

Dynamic studies of legs are not frequent

65 cm bore (just above PET-MR) large solid angle
→ suitable for nearly all Euro/Asian patients
→ 25 % less detector

Monolithic detector technology has DOI
→ Full bore can be imaged with unifor tion

Thin detectors: better spatial resolutio OF

This talk: Cost and Sensit
1m and 2m versus 2

EANM 2017

Long Axial FOV – Total Body PET

- UC Davies
  - 2 m AxFOV with 25-50 x NEC high sensitivity
  - TOF and DOI essential

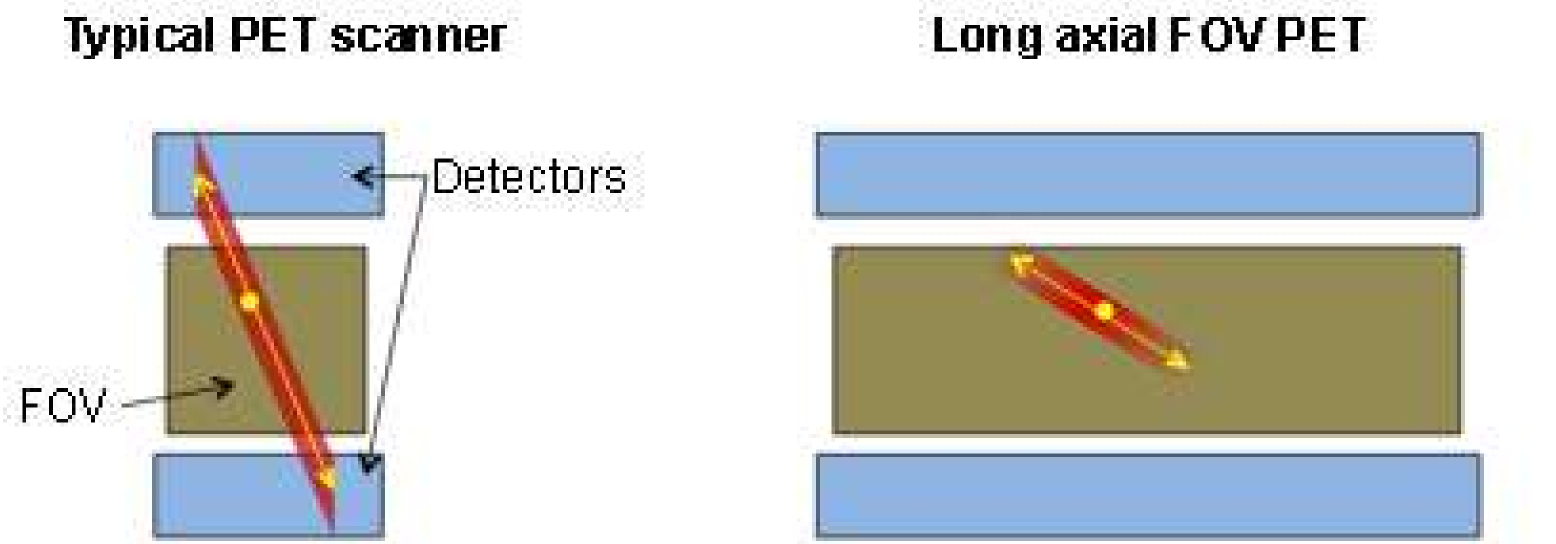

Total Body PET: The EXPLORER Project

2m PET

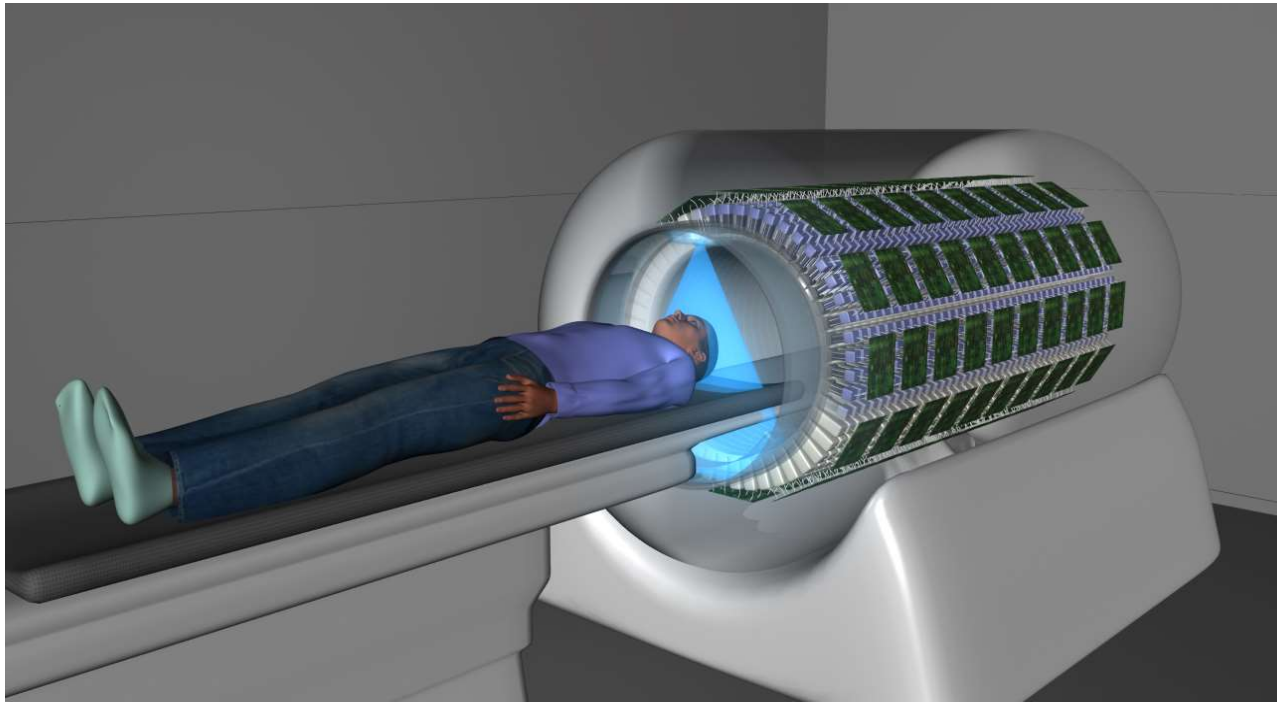

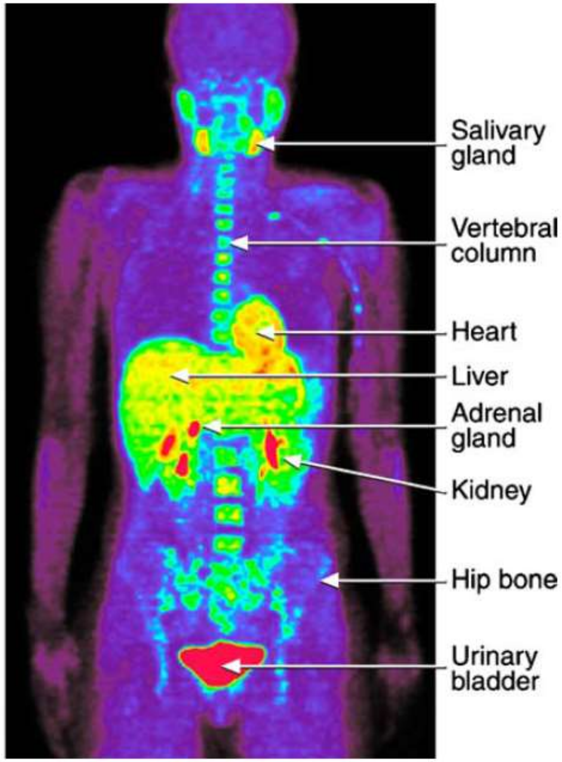

http://explorer.ucdavis.edu/

Total body PET – from mice to men

The first interactive, multidisciplinary conference focused on new technology and systems, fast, dynamic imaging and low dose applications of Total Body PET in animal science and medicine.

The Total Body PET conference 2018 is organized by Ghent University and the Ghent University Hospital. June 30 – July 2, 2018, Thagaste, Ghent (Belgium)

Siemens Biograph Vision Quadra

Quadra room at Turku PET Centre. A 106 cm z-axis scanner installation in April 2022

[Biograph Vision Quadra (siemens-healthineers.com)](https://www.siemens-healthineers.com/molecular-imaging/pet-ct/biograph-vision-quadra)

https://www.siemens-healthineers.com/molecular-imaging/pet-ct/biograph-vision-quadra

❑ Turku PET group

- Juhani Knuuti – the driving force
- Tuula Tolvanen – Phantoms
- Mika Teräs – On the background
- Hidehiro Iida – Perfusion etc
- Virva Saunavaara – PET/MR, TB PET
- Jarmo Teuho – Corrections
- Riku Klen – Motion correction
- Jani Linden – reconstruction algorithms
- + Many More

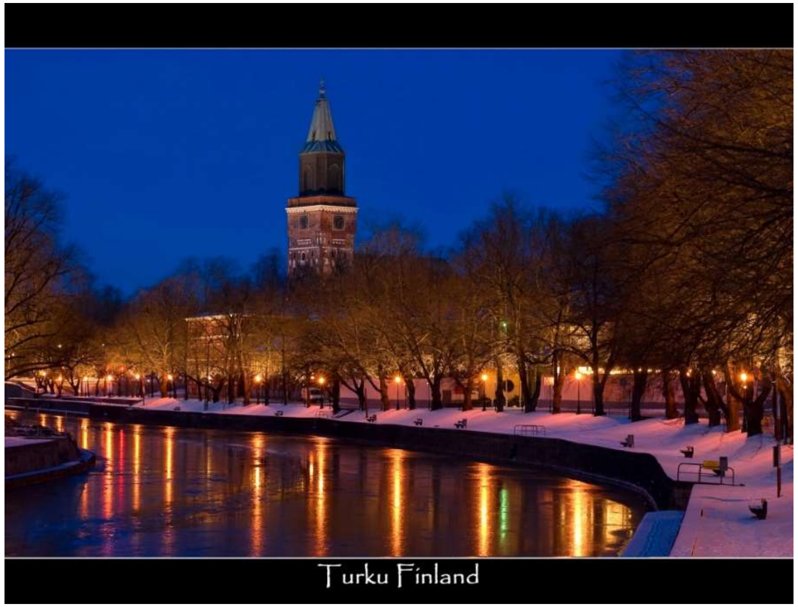

❑ Collaborators

- Eero Lehtonen, Future Technologies, UTU
- Mojtaba Jafari Tadi, TU Applied Sciences
- Kris Thielemans, Brian Hutton, UCL London
- Ronald Boellaard, VU Amsterdam
- Valentino Bettinardi, HSR Milan
- Thomas Beyer, MUV, Vienna

❑ Master Research Agreements with TUH

- **GEHC**
- **Siemens**
- **Philips**

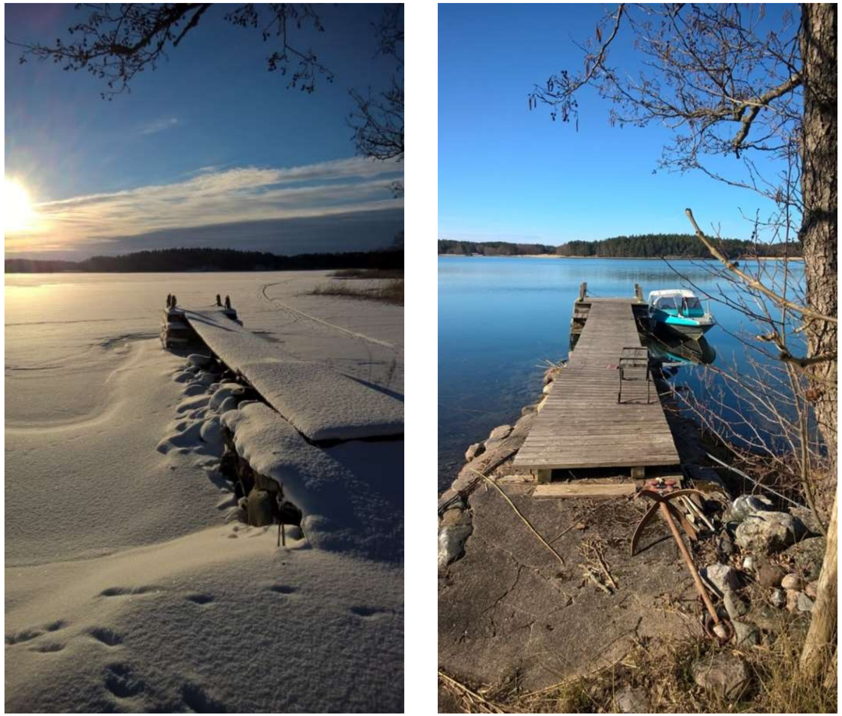

Thank you for your attention !

60°.51, 21°.35